Remote Sensing of Vegetation

Carolina Distinguished Professor
Department of Geography
University of South Carolina
Columbia, South Carolina 29208
jrjensen@sc.edu

Remote Sensing of Vegetation

Spectral Characteristics

Dominant Factors Controlling Leaf Reflectance

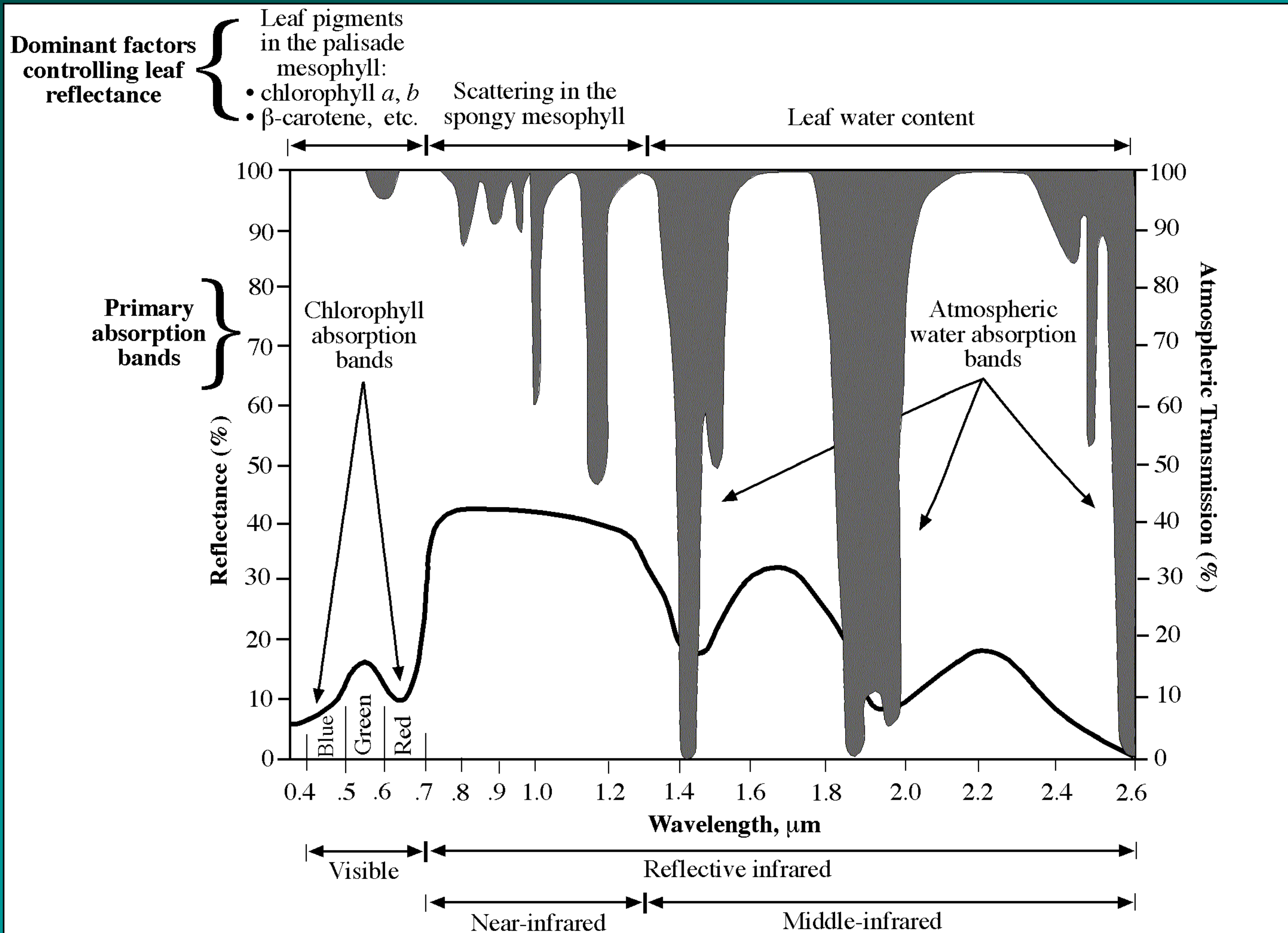

Water absorption bands:
0.97 μm
1.19 μm
1.45 μm
1.94 μm
2.70 μm

Jensen, 2000

Cross-section Through A Hypothetical and Real Leaf Revealing the Major Structural Components that Determine the Spectral Reflectance of Vegetation

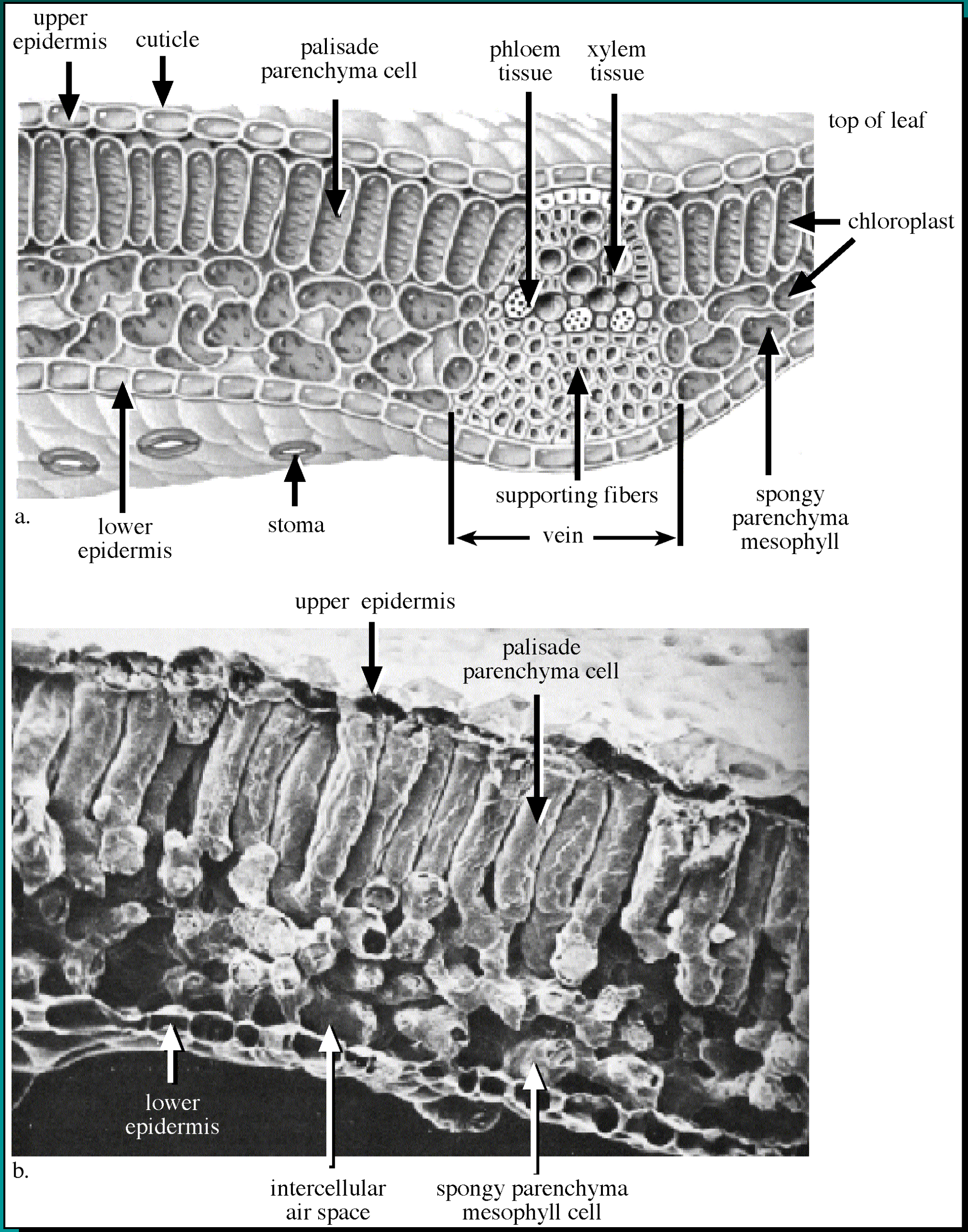

Jensen, 2000

Absorption Spectra of Chlorophyll *a* and *b*, *β*-carotene, Pycoerythrin, and Phycocyanin Pigments

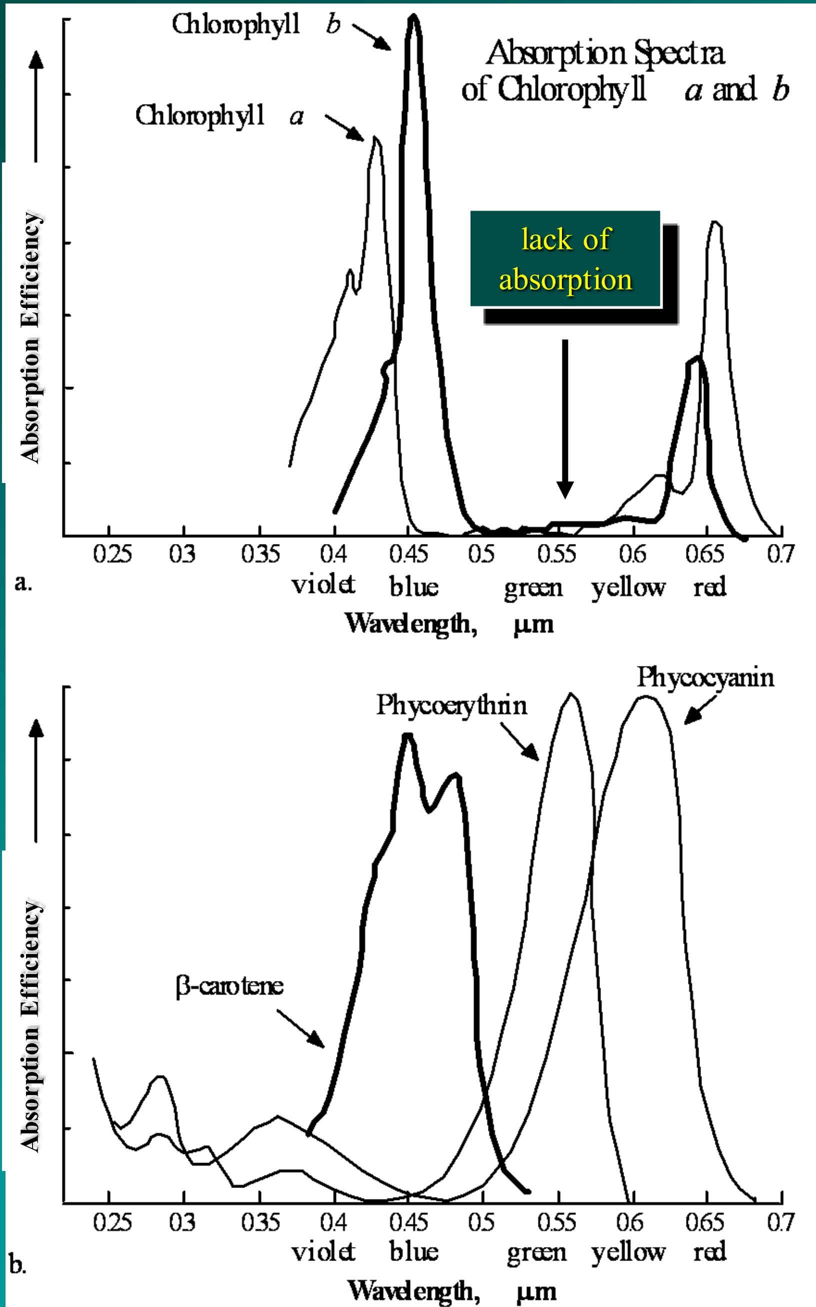

Chlorophyll *a* peak absorption is at 0.43 and 0.66 µm.

Chlorophyll *b* peak absorption is at 0.45 and 0.65 µm.

Optimum chlorophyll absorption windows are:
0.45 - 0.52 µm and 0.63 - 0.69 µm

Jensen, 2000

Litton Emerge Spatial, Inc., CIR image (RGB = NIR,R,G) of Dunkirk, NY, at 1 x 1 m obtained on December 12, 1998.

Natural color image (RGB = RGB) of a N.Y. Power Authority lake at 1 x 1 ft obtained on October 13, 1997.

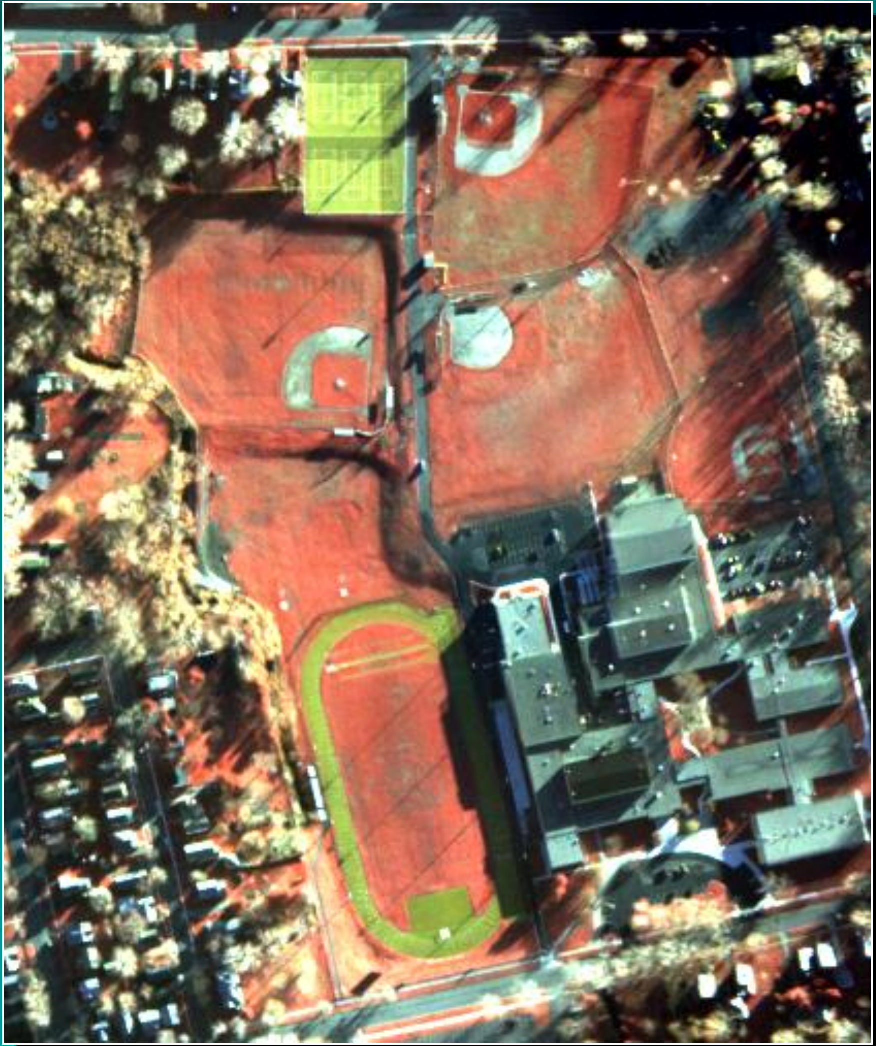

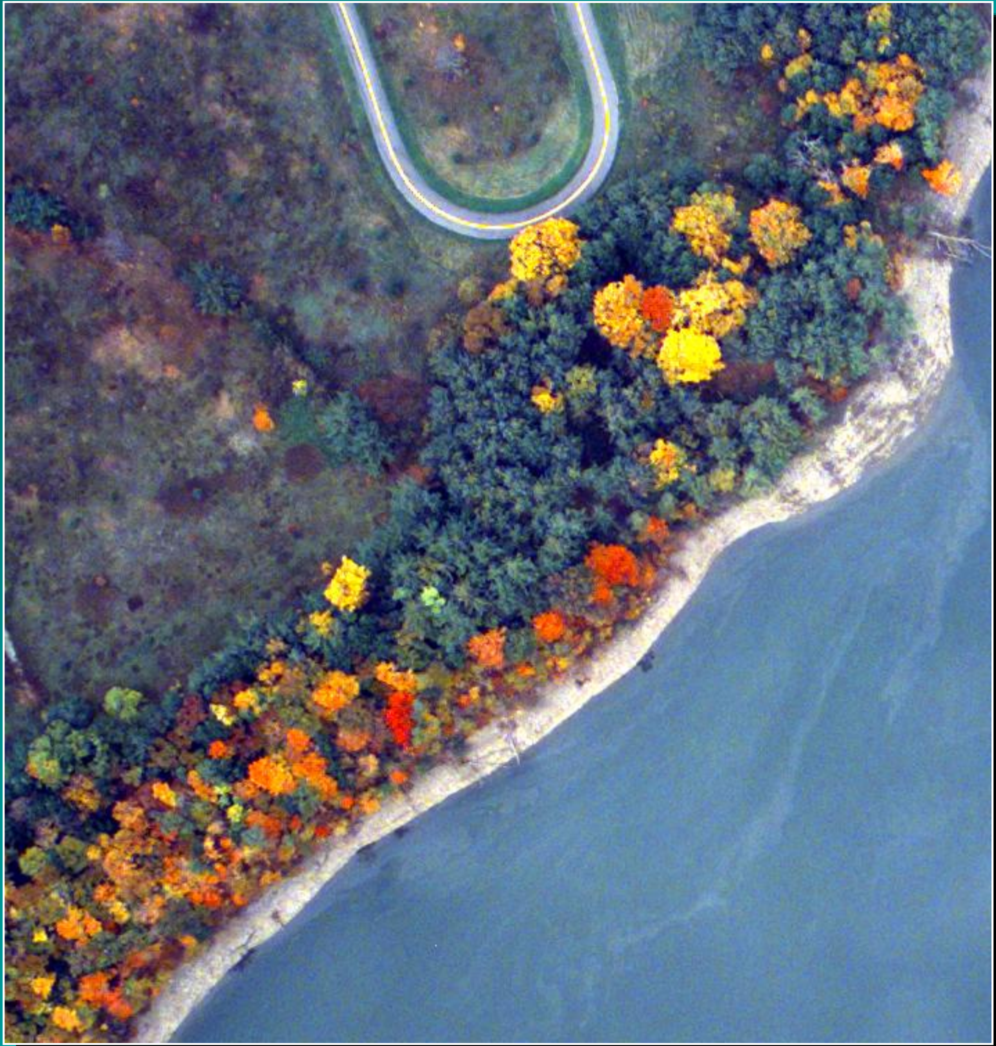

Spectral Reflectance Characteristics of Sweetgum Leaves (*Liquidambar styraciflua* L.)

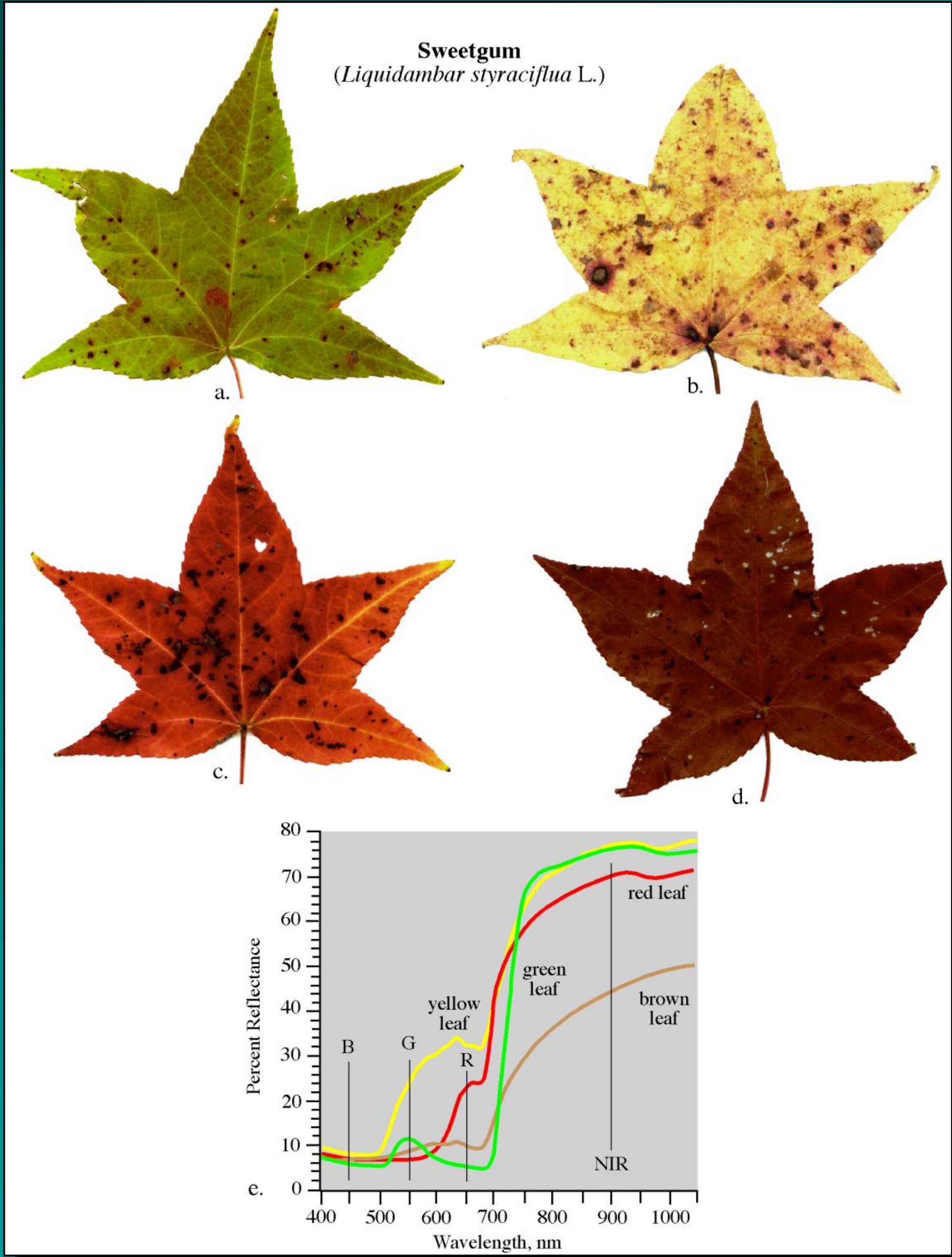

Jensen, 2000

Spectral Reflectance Characteristics of Selected Areas of Blackjack Oak Leaves

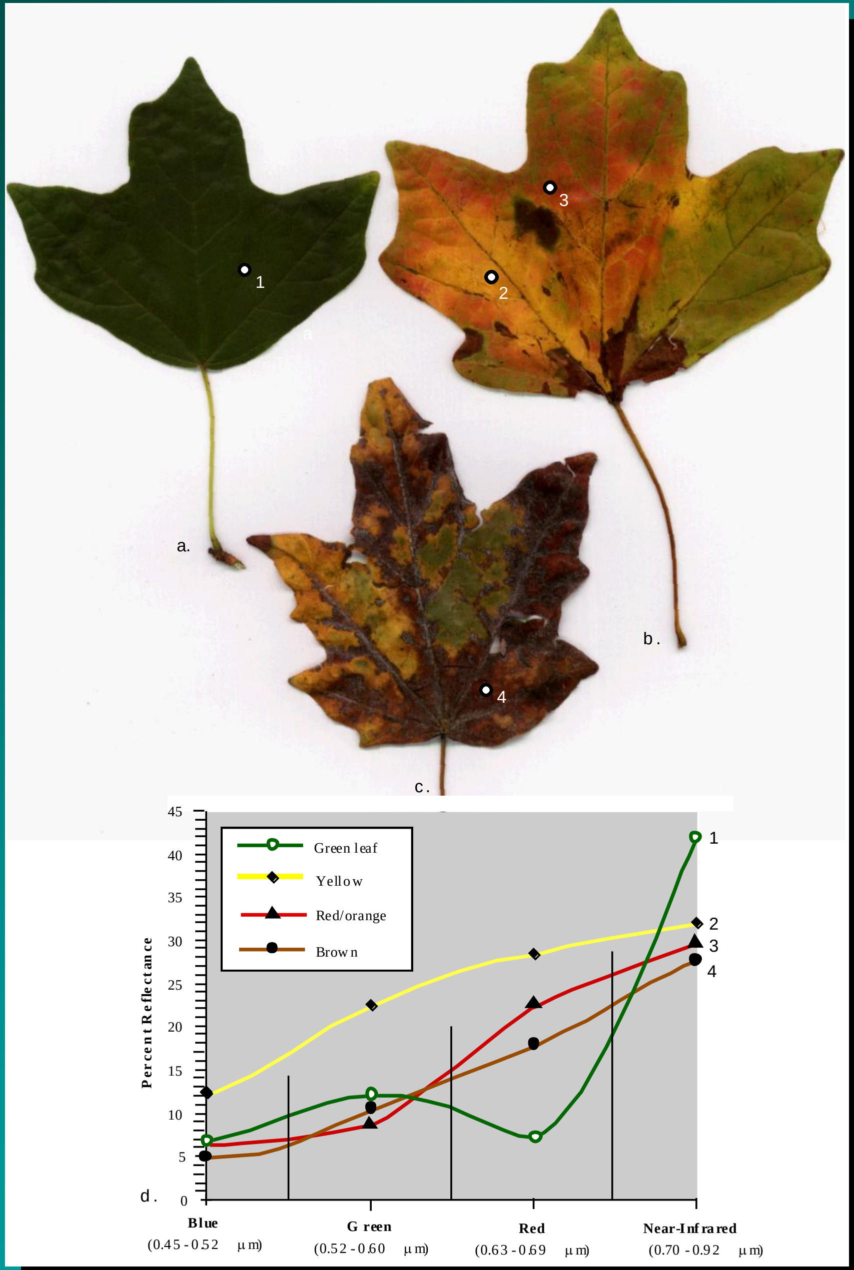

Jensen, 2000

Hemispherical Reflectance, transmittance, and Absorption Characteristics of Big Bluestem Grass

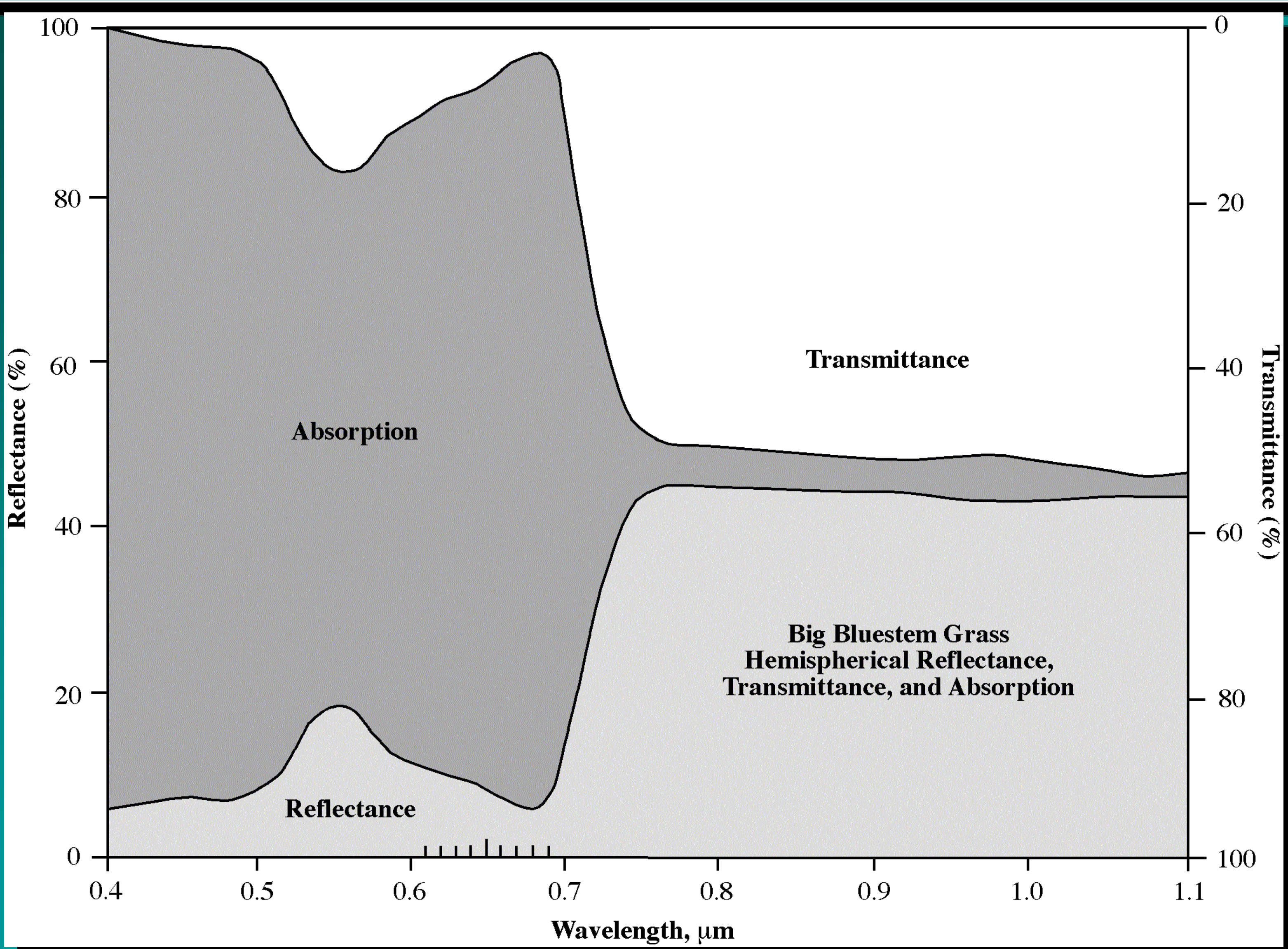

Jensen, 2000

Hypothetical Example of Additive Reflectance from A Canopy with Two Leaf Layers

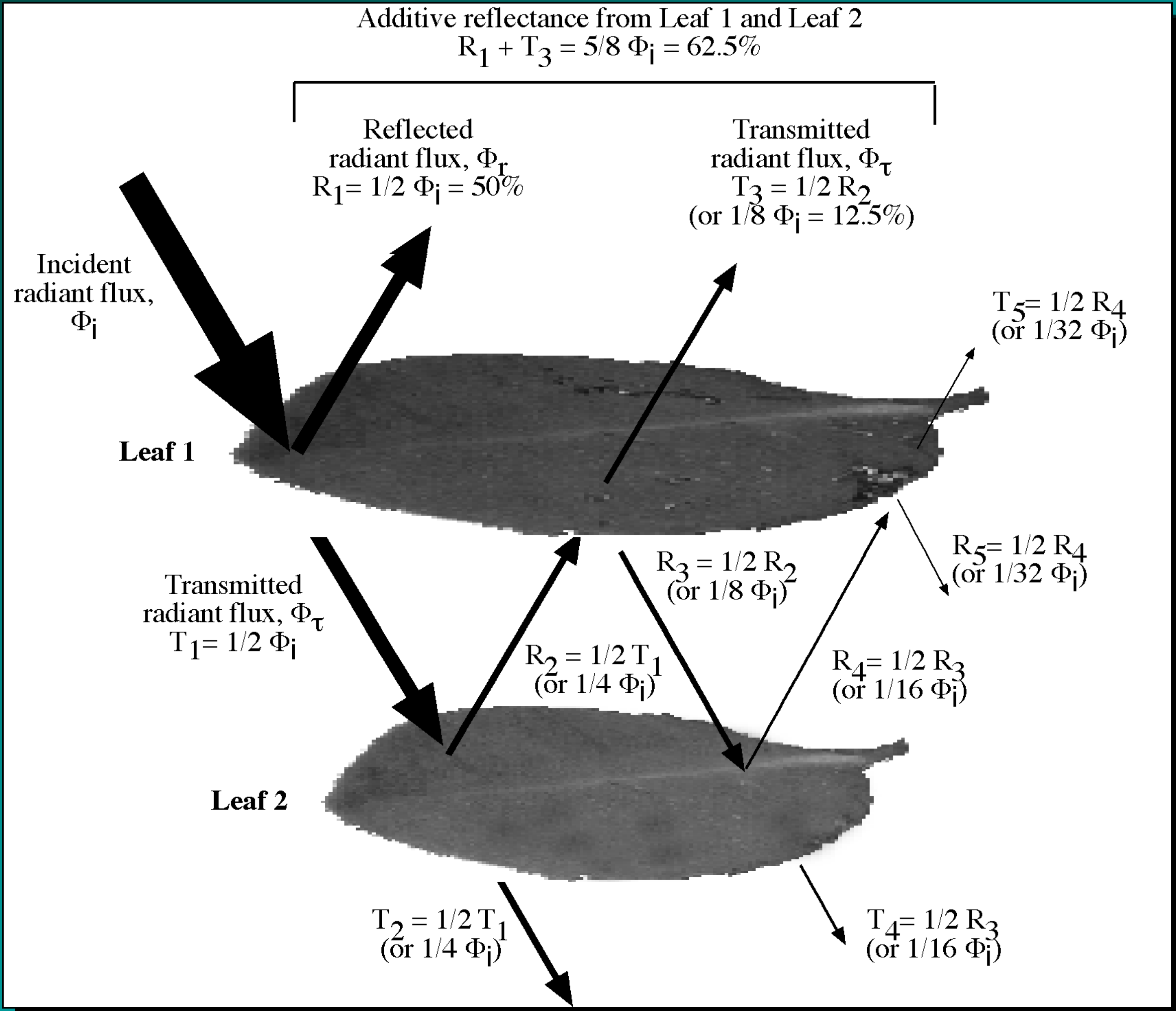

Jensen, 2000

Distribution of Pixels in a Scene in Red and Near-infrared Multispectral Feature Space

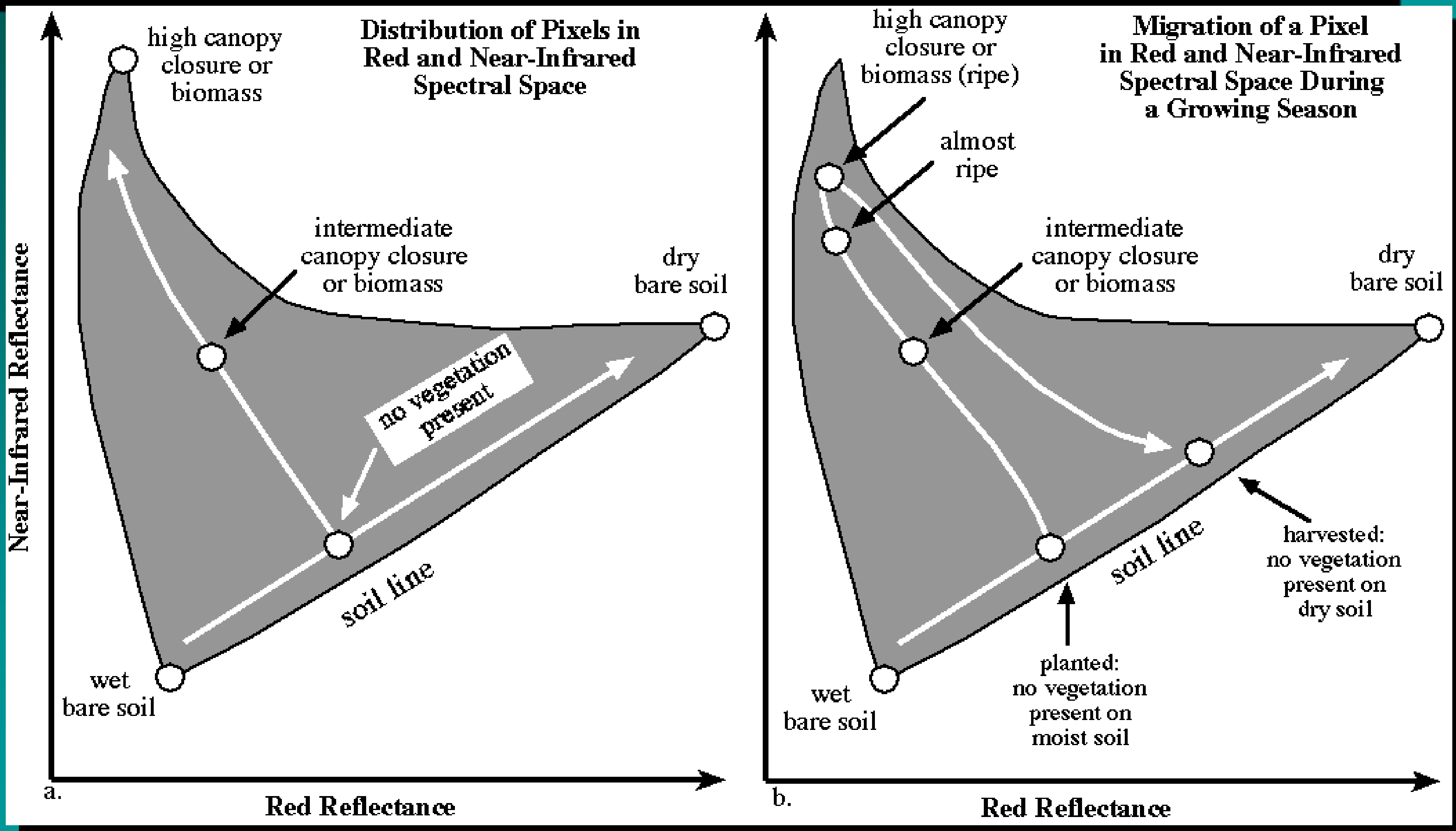

Jensen, 2000

Reflectance Response of a Single Magnolia Leaf (*Magnolia grandiflora*) to Decreased Relative Water Content

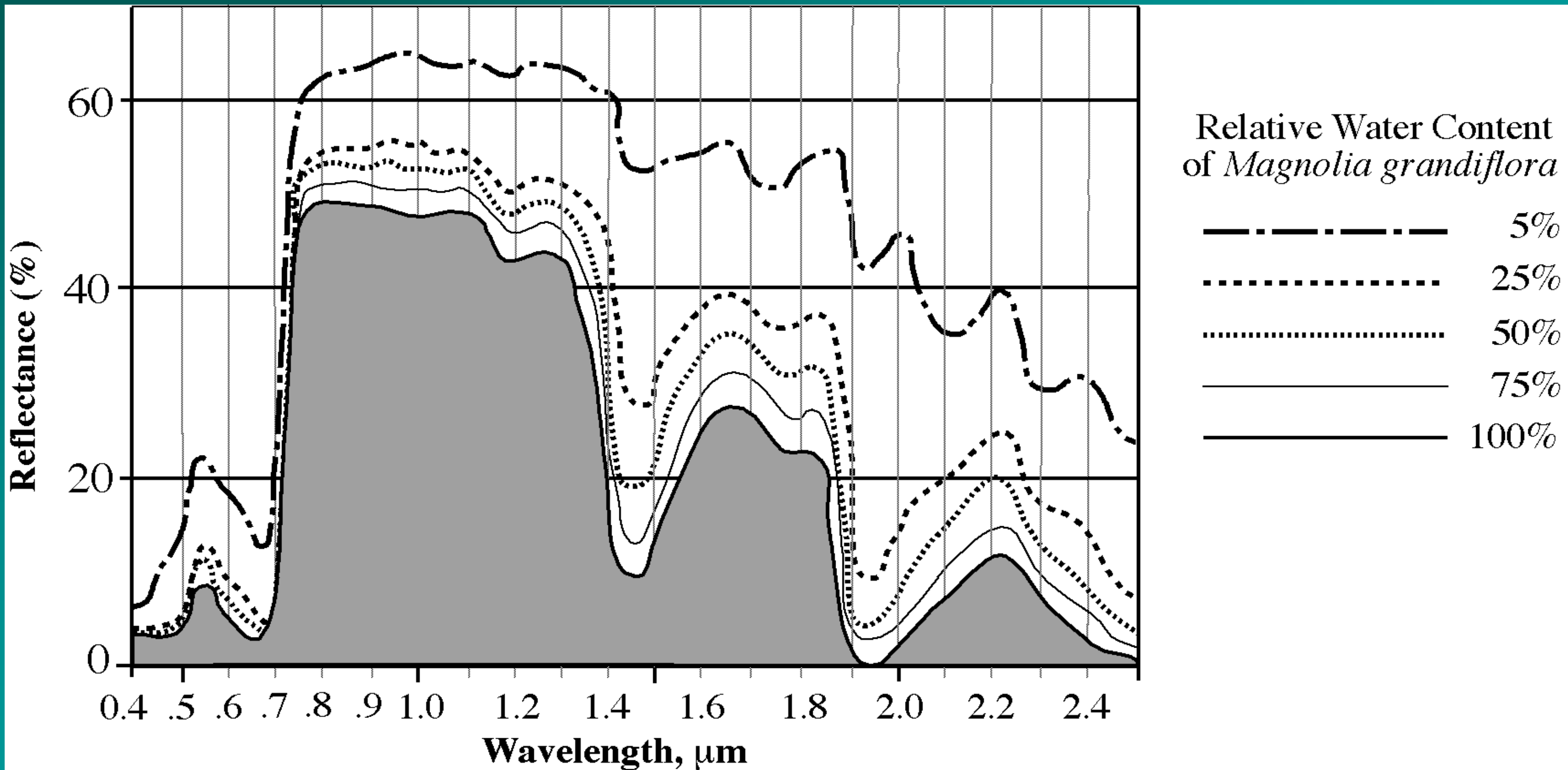

Jensen, 2000

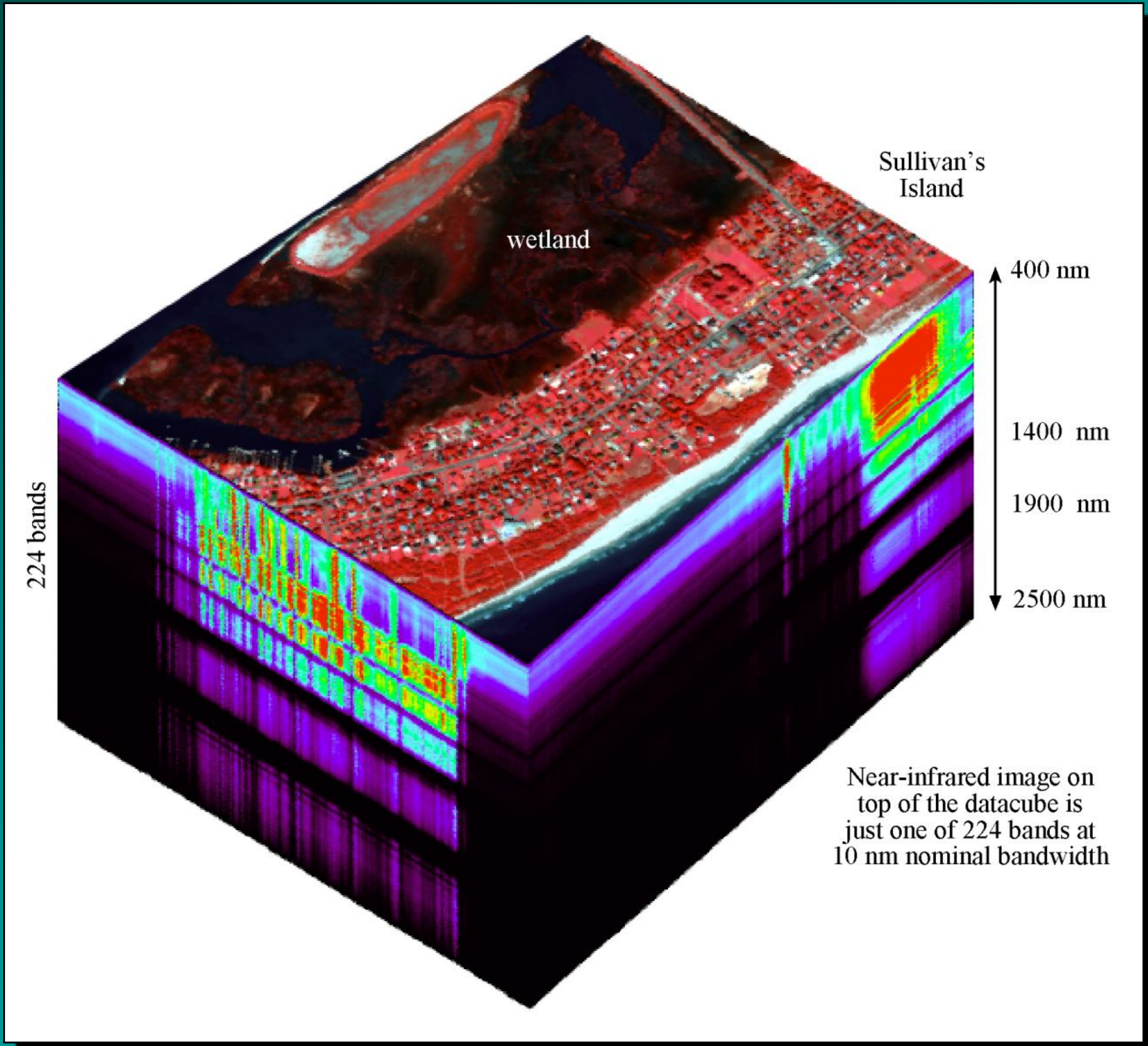

Airborne Visible Infrared Imaging Spectrometer (AVIRIS) Datacube of Sullivan's Island Obtained on October 26, 1998

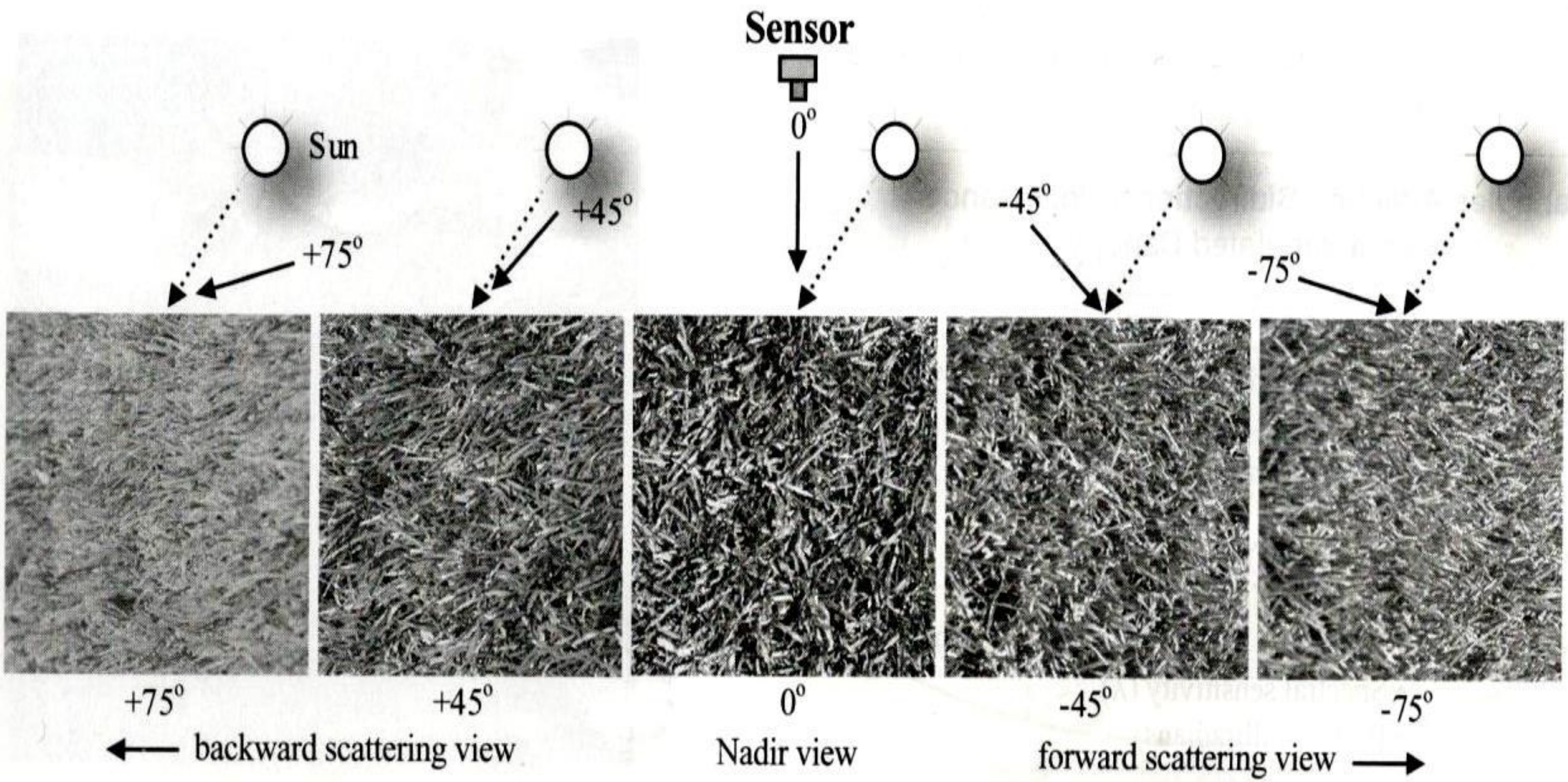

re 11-8 The bidirectional reflectance effect on a field of ryegrass (*Lolium perenne L.*) observed under different viewing angles in the solar principal plane from a FIGOS mounted camera. Solar zenith angle was at 35° as indicated by the dashed arrows. The sensor viewing angles are shown as black lines at nadir (0°) and at ±45° and ±75° off-nadir (after Sandmeier and Itten, 1999).

Imaging Spectrometer Data of Healthy Green Vegetation in the San Luis Valley of Colorado Obtained on September 3, 1993 Using AVIRIS

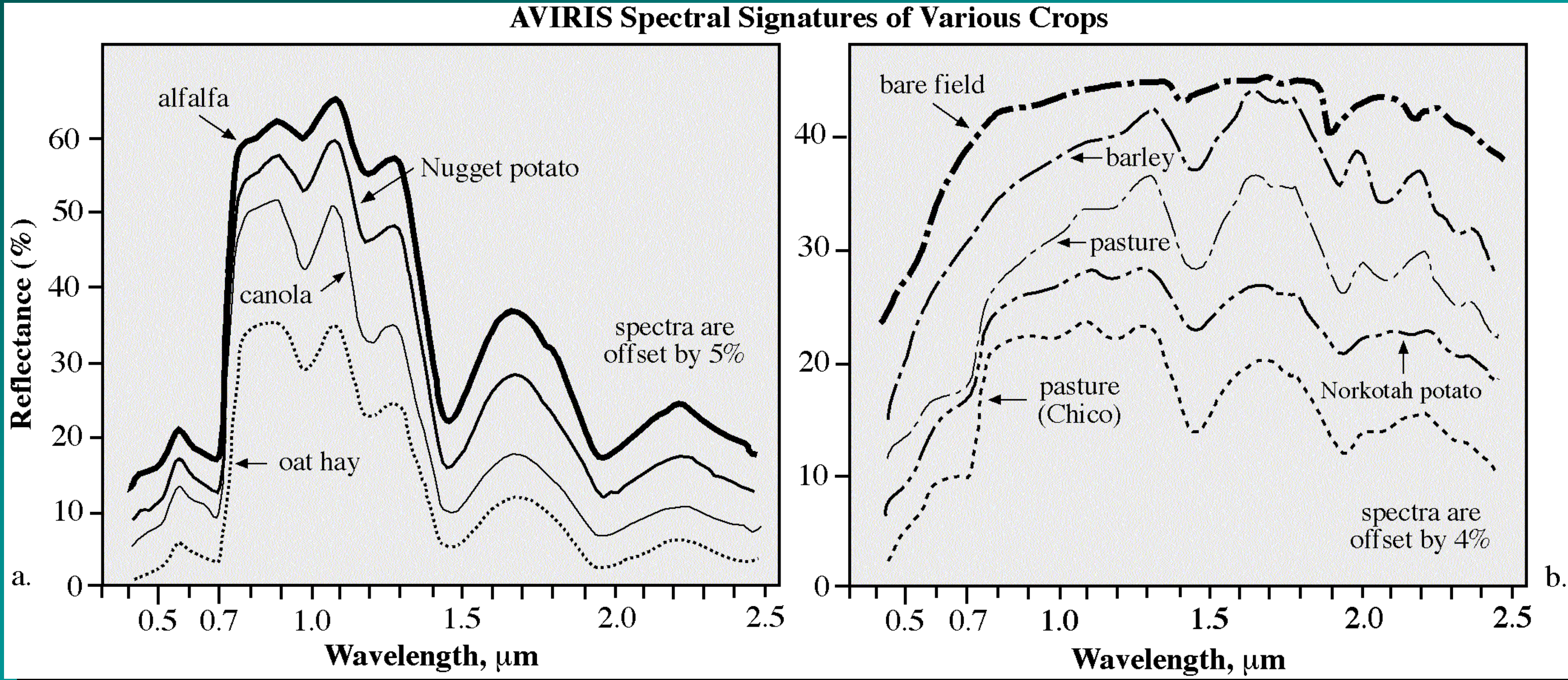

224 channels each 10 nm wide with 20 x 20 m pixels

Jensen, 2000

Hyperspectral Analysis of AVIRIS Data Obtained on September 3, 1993 of San Luis Valley, Colorado

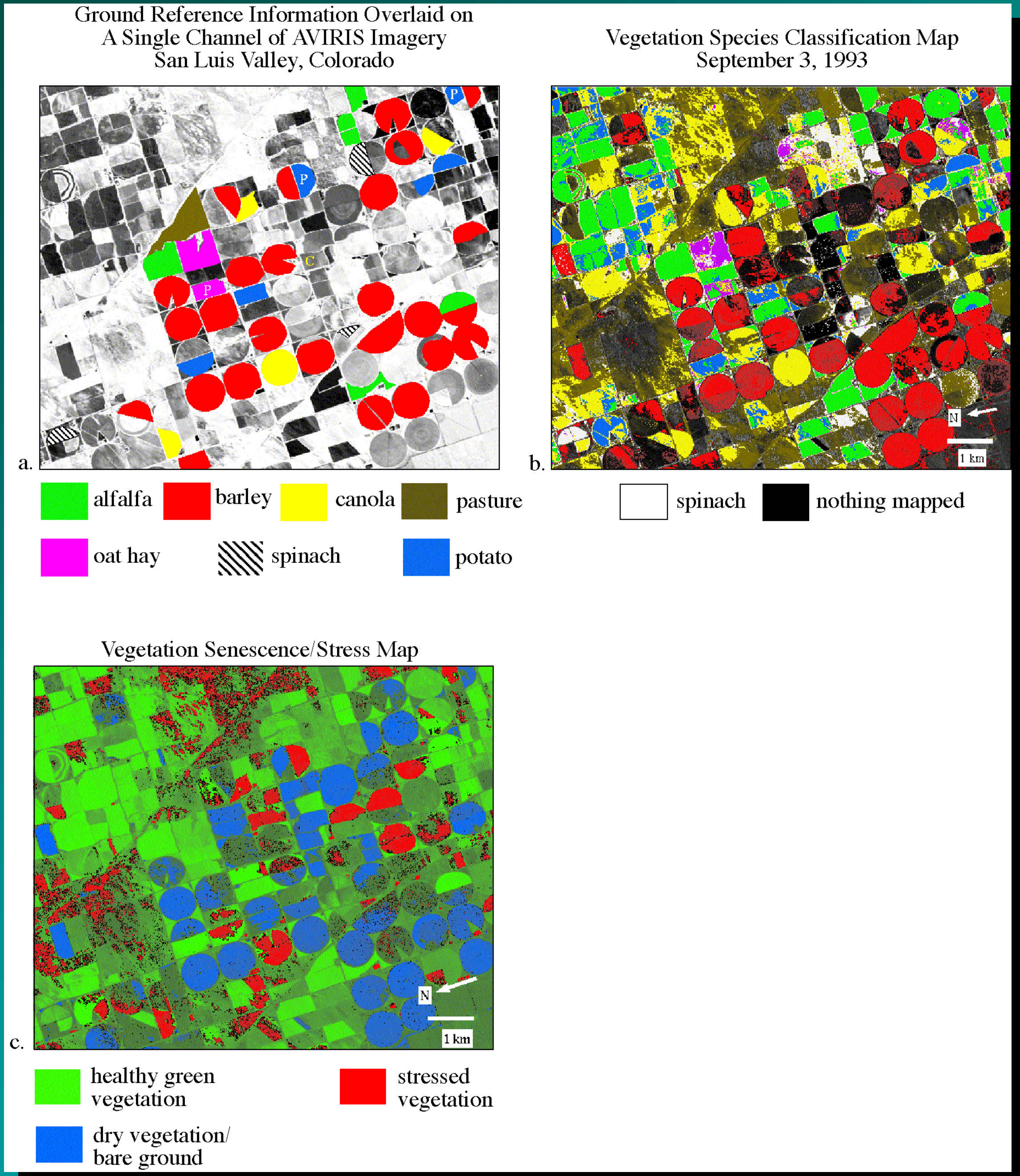

Jensen, 2000

Goniometer in Operation at North Inlet, SC

Jensen, 2000

Temporal (Phenological) Characteristics

Predicted Percent Cloud Cover in Four Areas in the United States

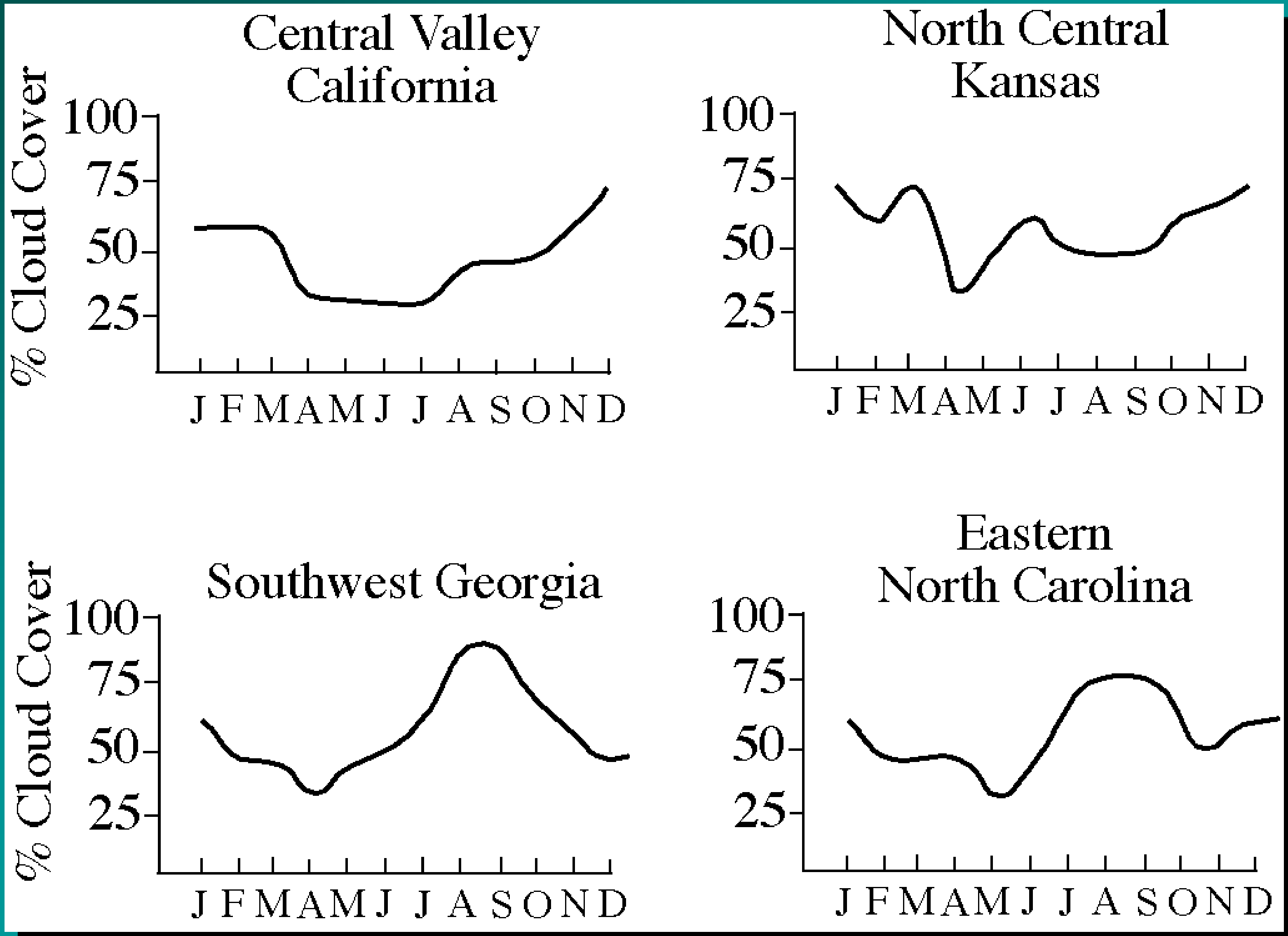

Jensen, 2000

Phenological Cycle of Hard Red Winter Wheat in the Great Plains

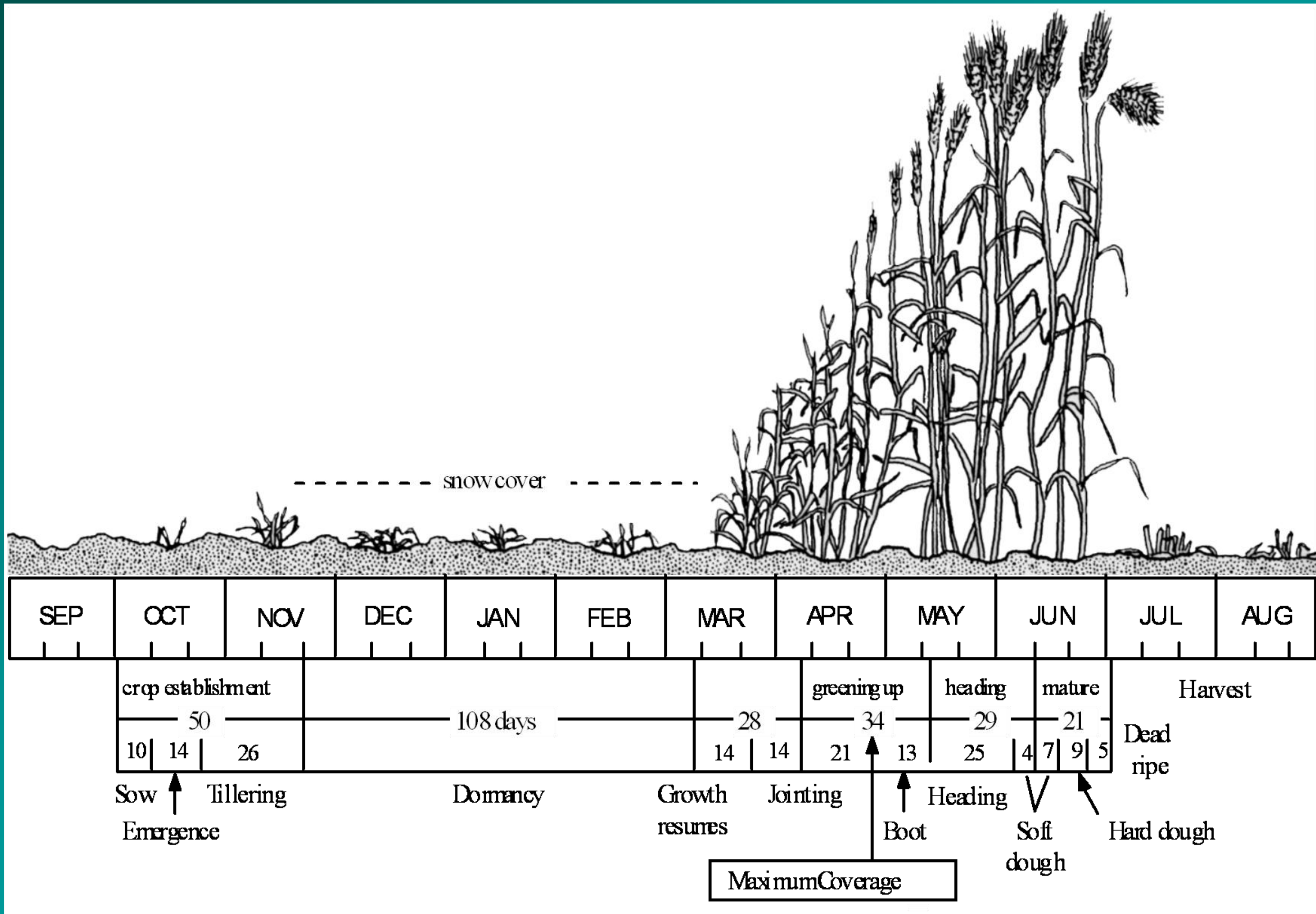

Jensen, 2000

Phenological Cycles of San Joaquin and Imperial Valley, California Crops and Landsat Multispectral Scanner Images of One Field During A Growing Season

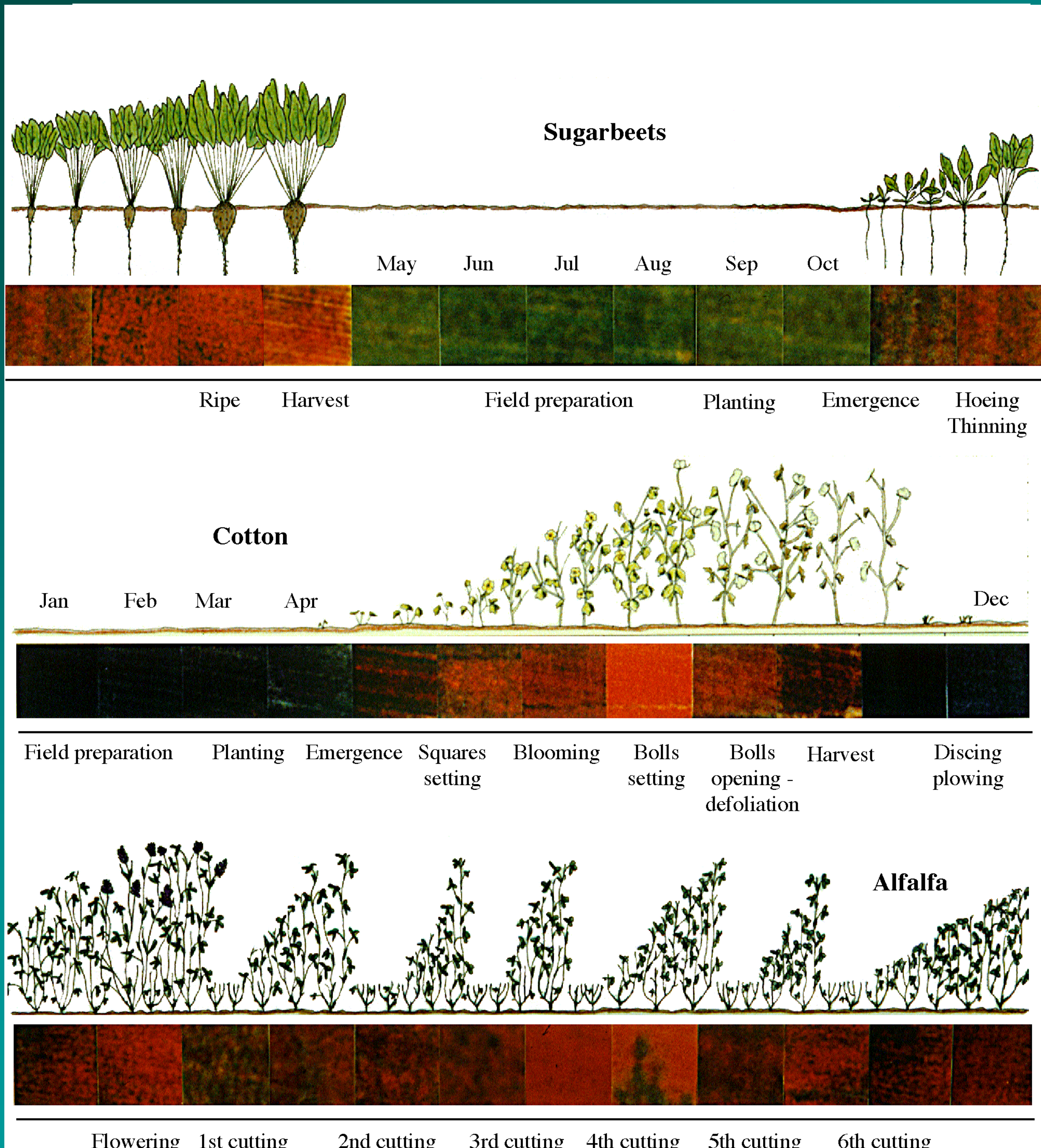

Jensen, 2000

Landsat Thematic Mapper Imagery of the Imperial Valley, California Obtained on December 10, 1982

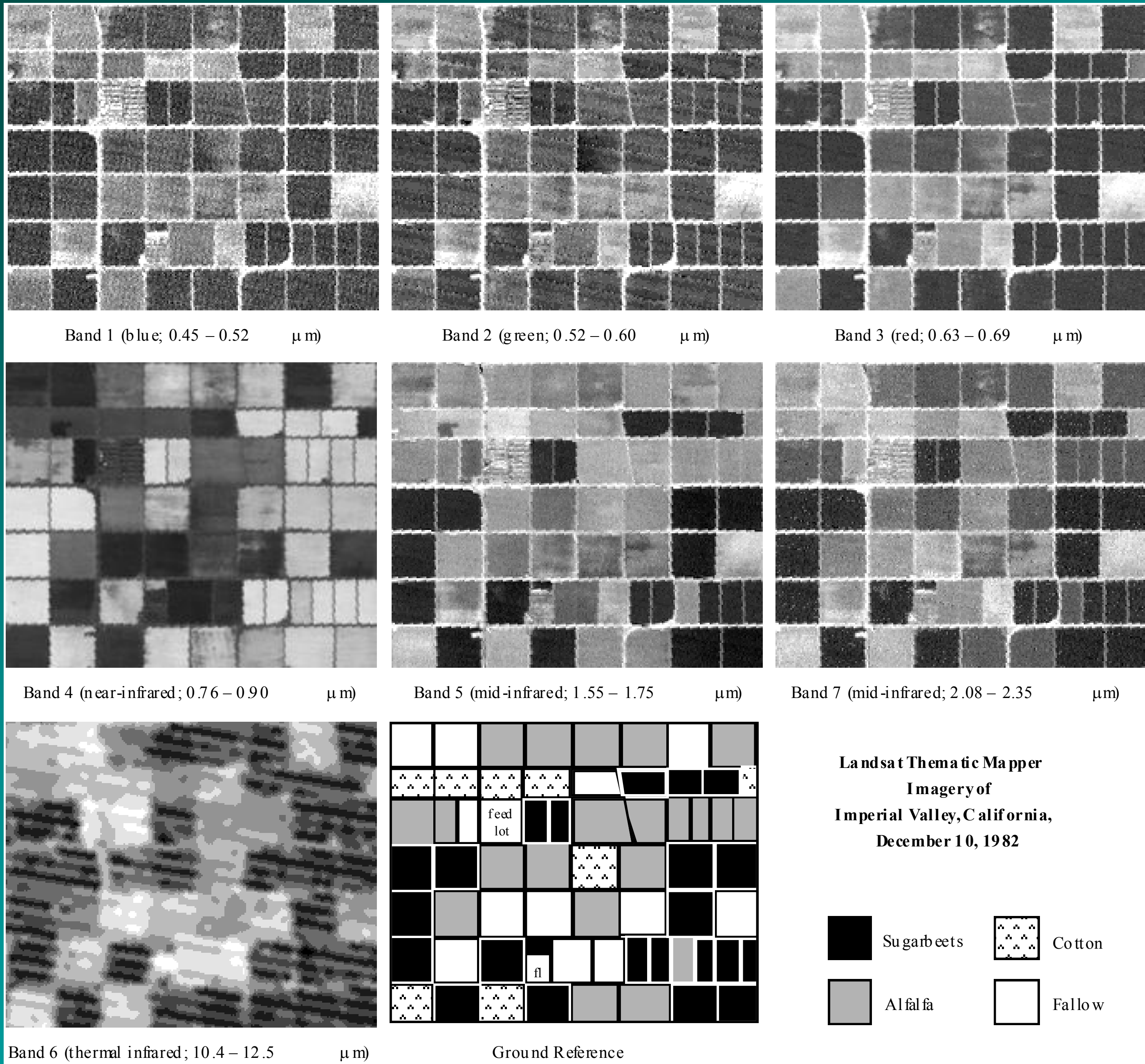

Jensen, 2000

Landsat Thematic Mapper Color Composites and Classification Map of a Portion of the Imperial Valley, California

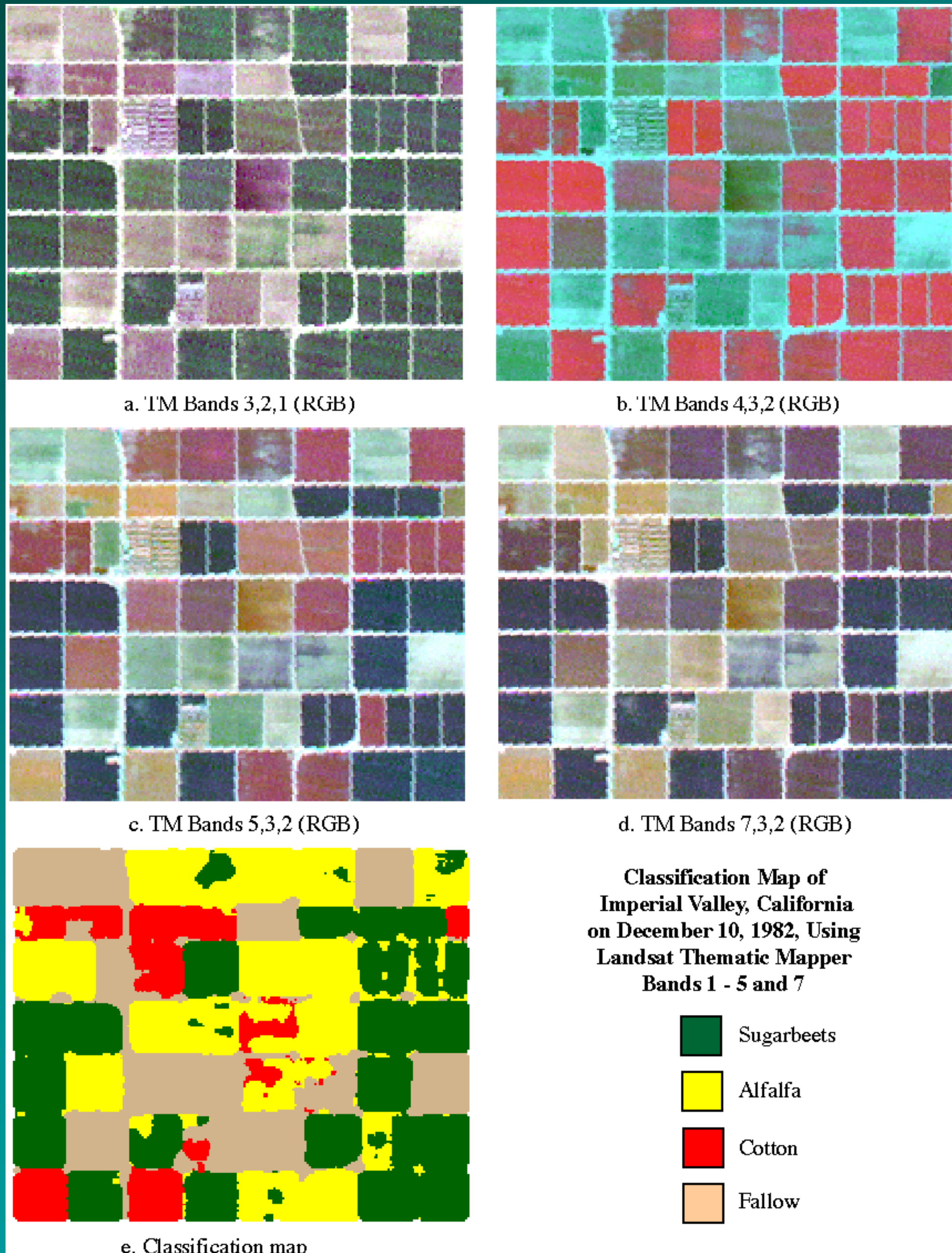

Jensen, 2000

Phenological Cycles of Soybeans and Corn in South Carolina

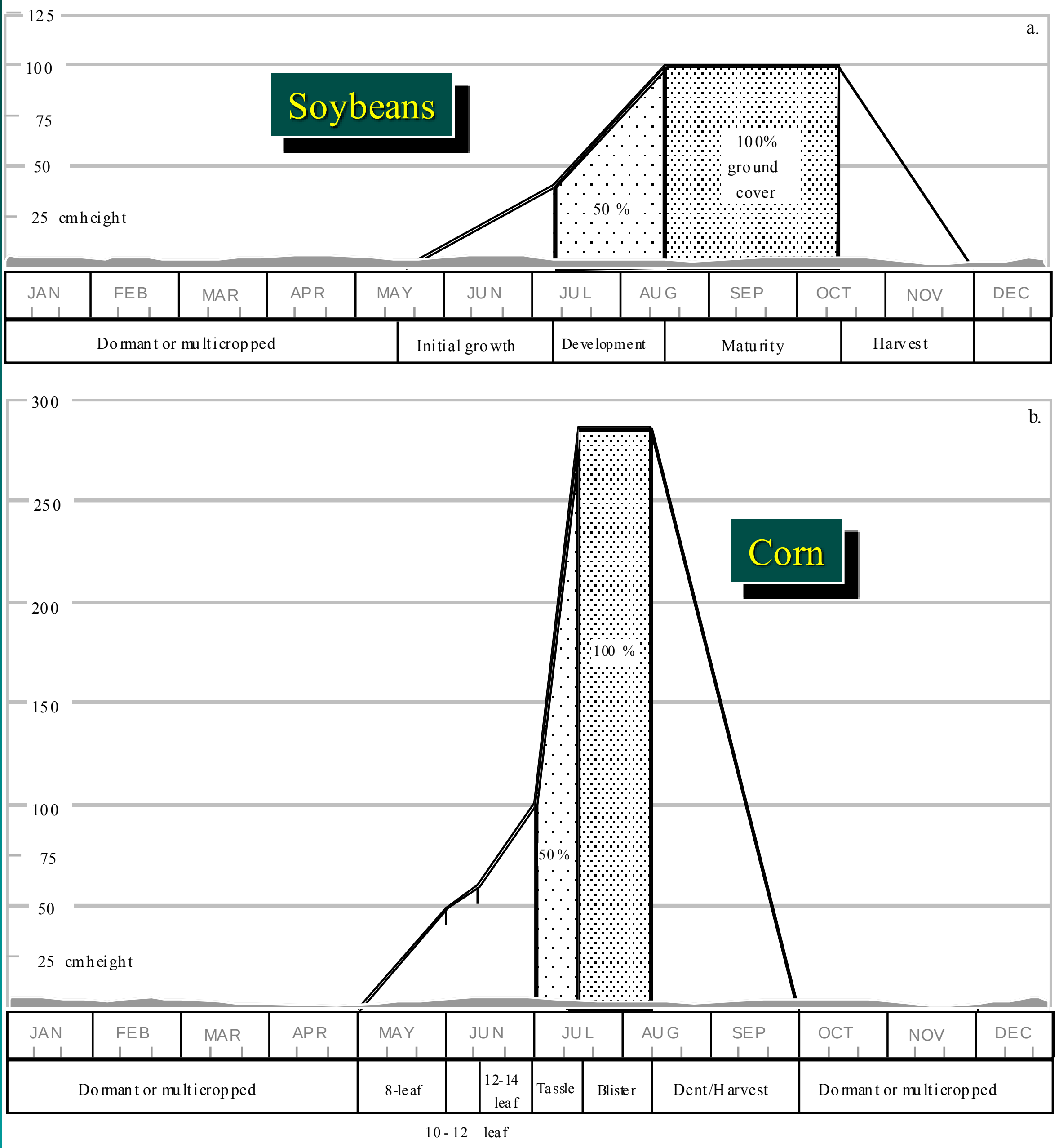

Jensen, 2000

Phenological Cycles of Winter Wheat, Cotton, and Tobacco in South Carolina

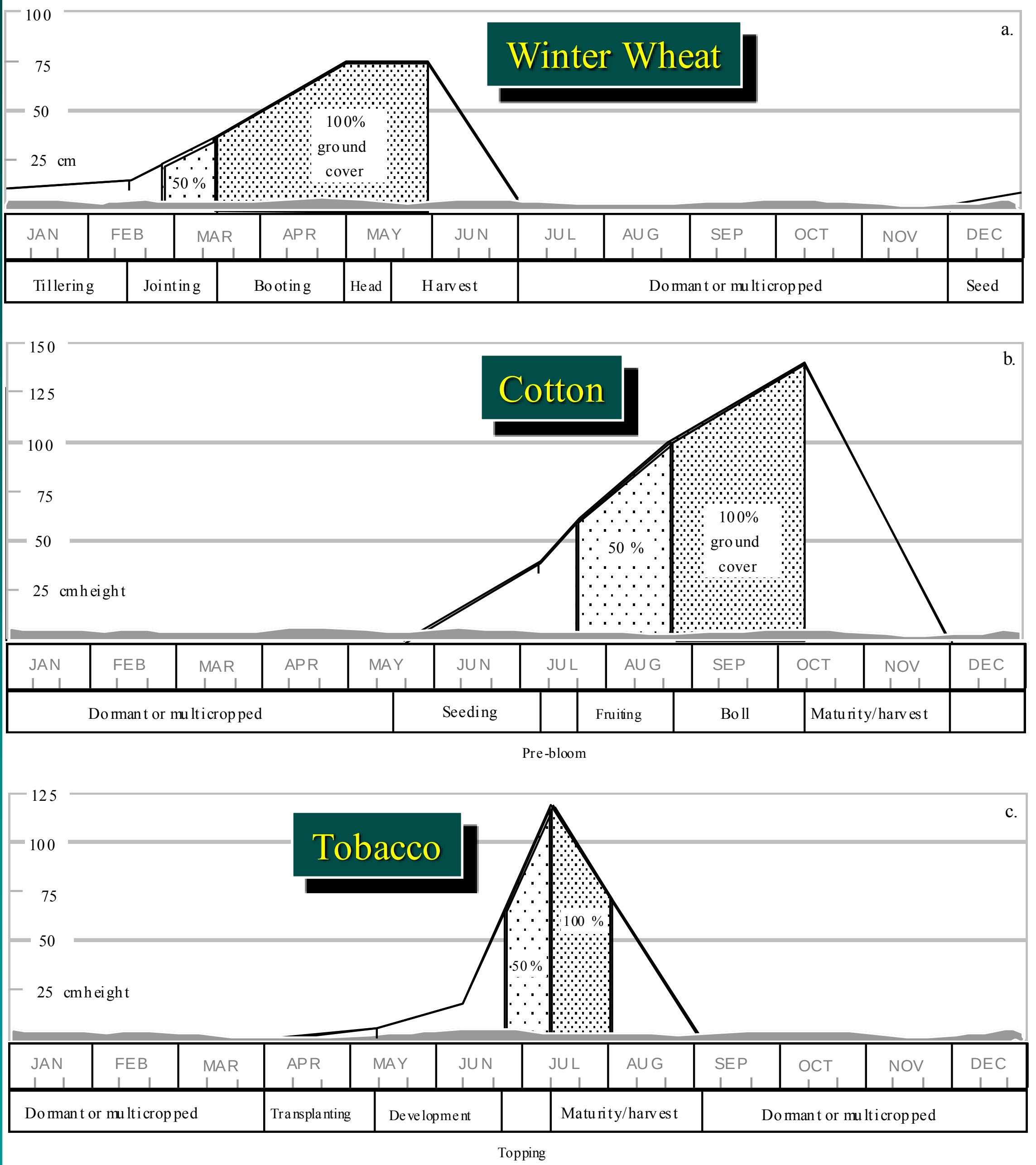

Jensen, 2000

Phenological Cycle of Cattails and Waterlilies in Par Pond, S.C.

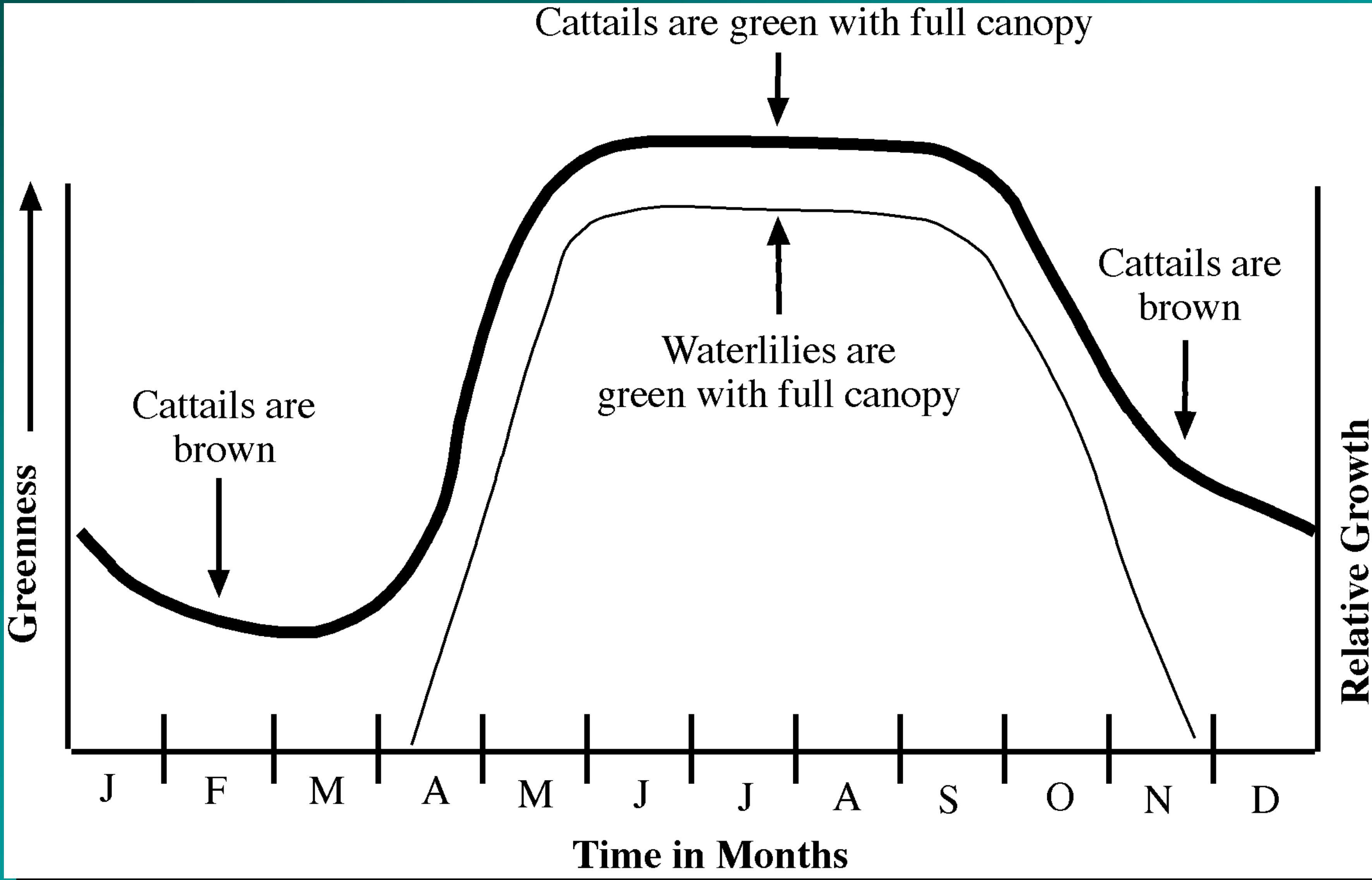

Jensen, 2000

Location of Murrells Inlet in South Carolina

Phenological Cycle of Smooth Cordgrass (*Spartina alterniflora*) Biomass in South Carolina

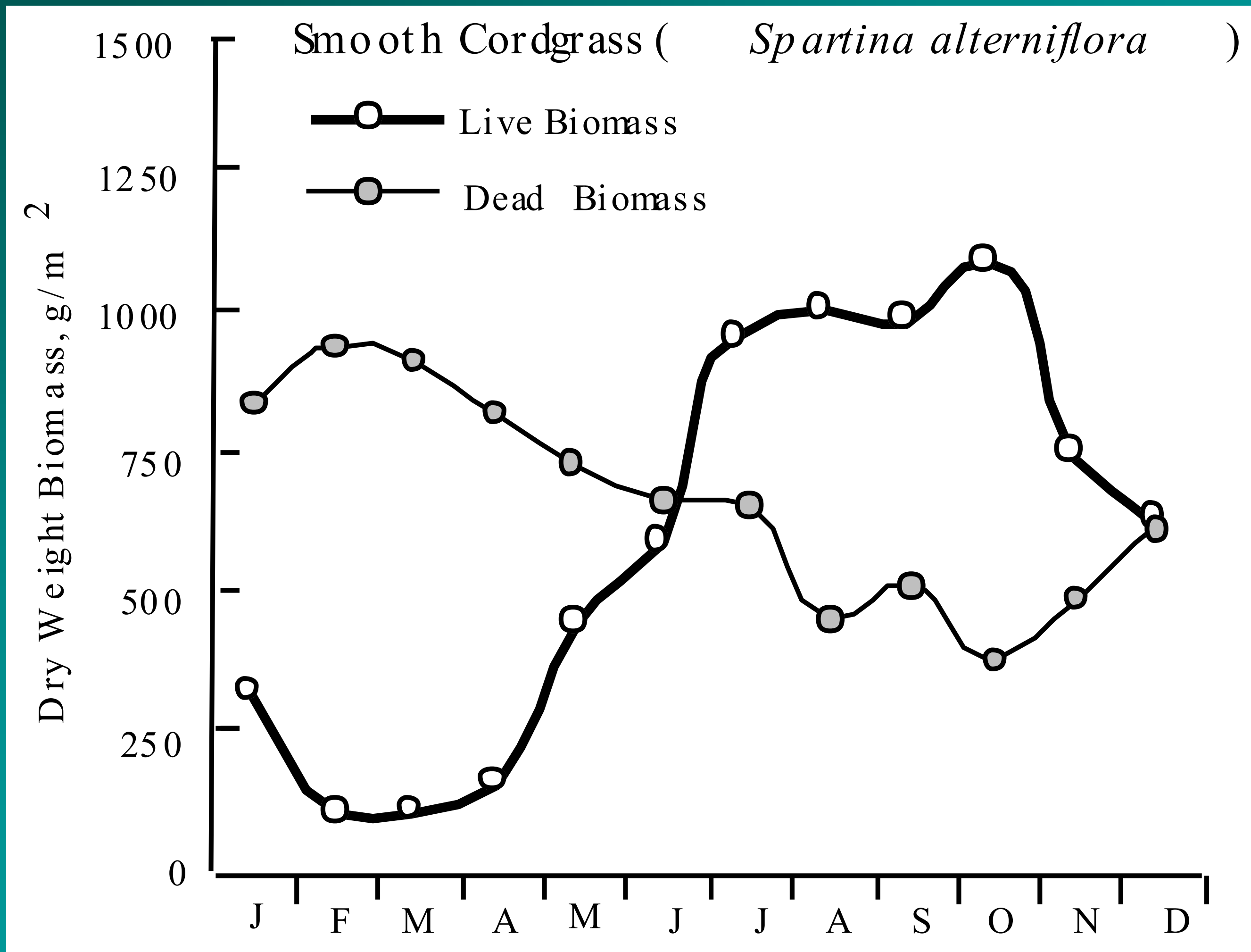

Jensen, 2000

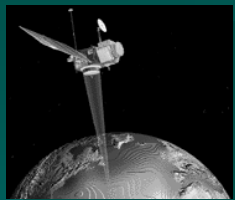

Characteristics of the NASA Calibrated Airborne Multispectral Scanner (CAMS) Mission of Murrells Inlet, S.C. on August 2, 1997

Mission Date	Visibility	Relative Humidity	Altitude above-ground-level	CAMS Spatial Resolution	CAMS Spectral Resolution
8/2/97	clear	45%	4000’	3.08 x 3.08	Band 1 (0.42 - 0.52 μm); blue
					Band 2 (0.52 - 0.60 μm); green
					Band 3 (0.60 - 0.63 μm); red
					Band 4 (0.63 - 0.69 μm); red
					Band 5 (0.69 - 0.76 μm); near-IR
					Band 6 (0.76 - 0.90 μm); near-IR
					Band 7 (1.55 - 1.75 μm); mid-IR
					Band 8 (2.08 - 2.35 μm); mid-IR
					Band 9 (10.5 - 12.5 μm); TIR

Nine Bands of 3 x 3 m Calibrated Airborne Multispectral Scanner (CAMS) Data of Murrells Inlet, SC Obtained on August 2, 1997

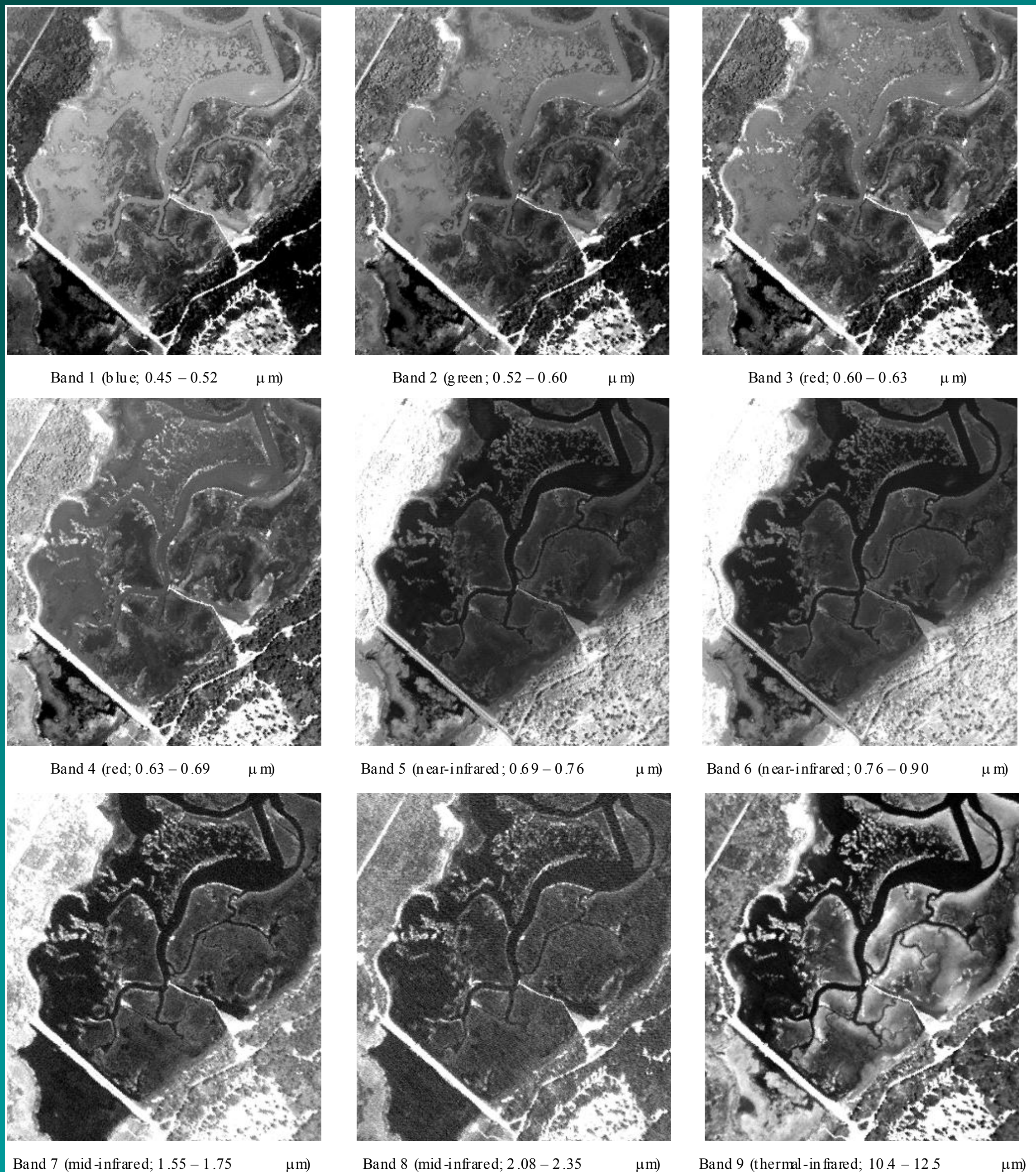

Band 1 (blue; 0.45 – 0.52 μm)
Band 2 (green; 0.52 – 0.60 μm)
Band 3 (red; 0.60 – 0.63 μm)
Band 4 (red; 0.63 – 0.69 μm)
Band 5 (near-infrared; 0.69 – 0.76 μm)
Band 6 (near-infrared; 0.76 – 0.90 μm)
Band 7 (mid-infrared; 1.55 – 1.75 μm)
Band 8 (mid-infrared; 2.08 – 2.35 μm)
Band 9 (thermal-infrared; 10.4 – 12.5 μm)

Jensen, 2000

Calibrated Airborne Multispectral Scanner Data of Murrells Inlet, S.C. Obtained on August 2, 1997

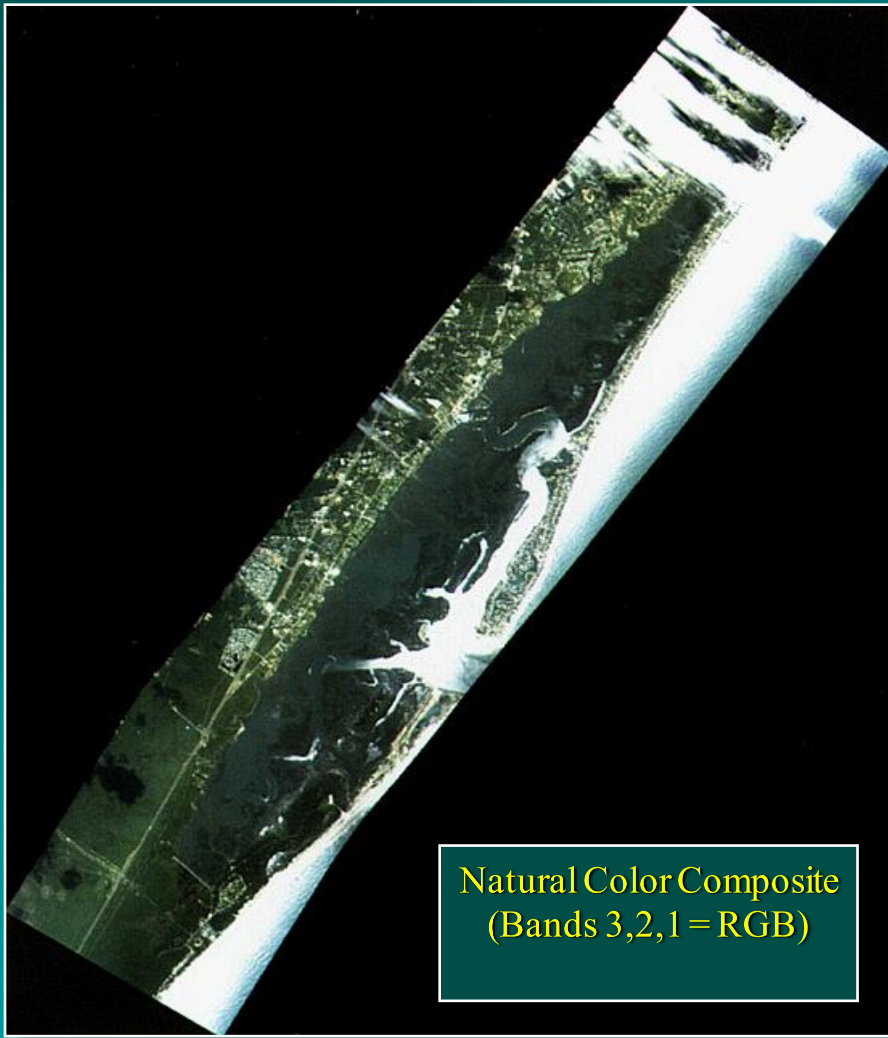

Natural Color Composite
(Bands 3,2,1 = RGB)

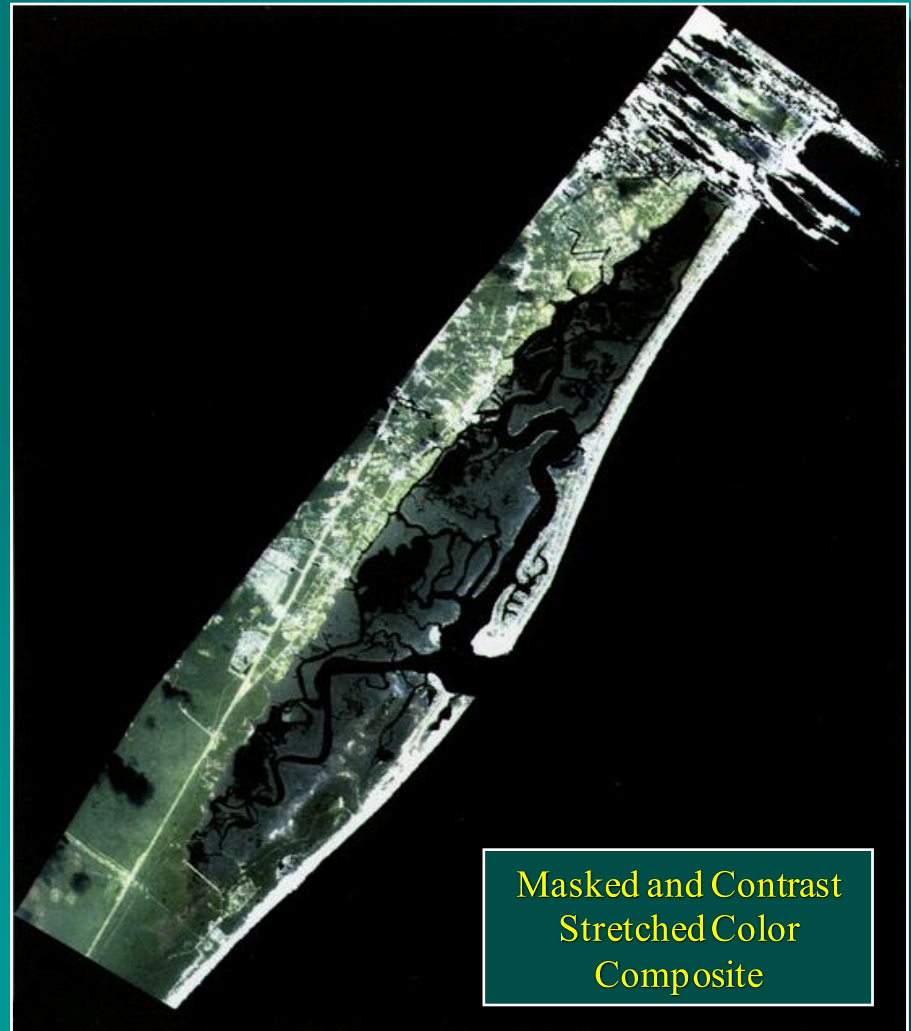

Masked and Contrast
Stretched Color
Composite

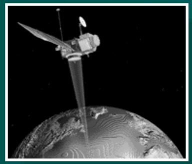

Calibrated Airborne Multispectral Scanner Data of Murrells Inlet, S.C. Obtained on August 2, 1997

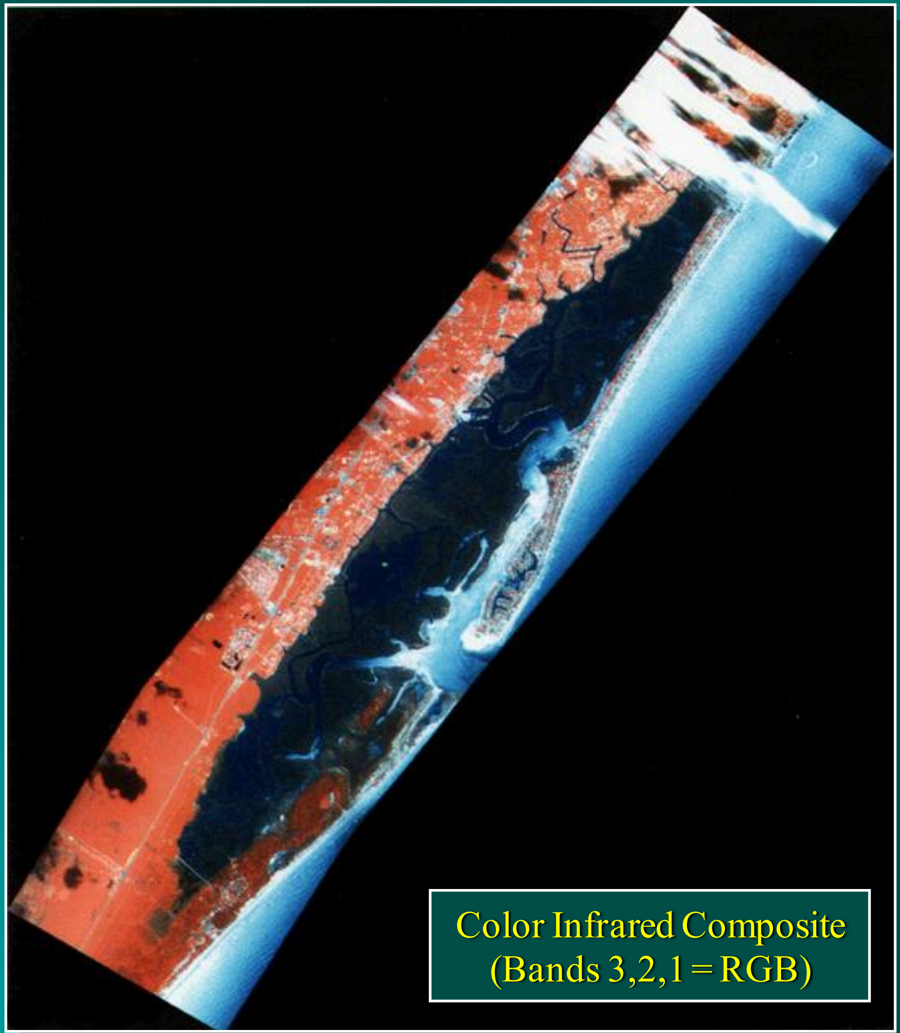

Color Infrared Composite (Bands 3,2,1 = RGB)

Masked and Contrast Stretched Color Composite

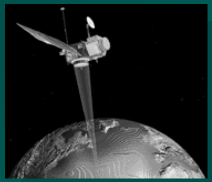

In Situ Ceptometer Leaf-Area-Index Measurement

- LAI may be computed using a Decagon Accupar Ceptometer™ that consists of a linear array of 80 adjacent 1 cm^2 photosynthetically active radiation (PAR) sensors along a bar.

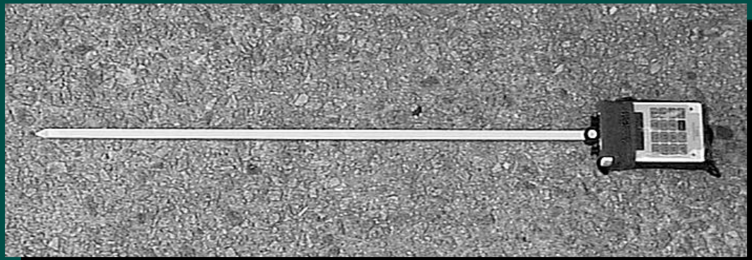

- Incident sunlight above the canopy, Q_a, and the amount of direct solar energy incident to the ceptometer, Q_b, when it was laid at the bottom of the canopy directly on the mud is used to compute LAI.

In Situ Ceptometer Leaf-Area-Index Measurement

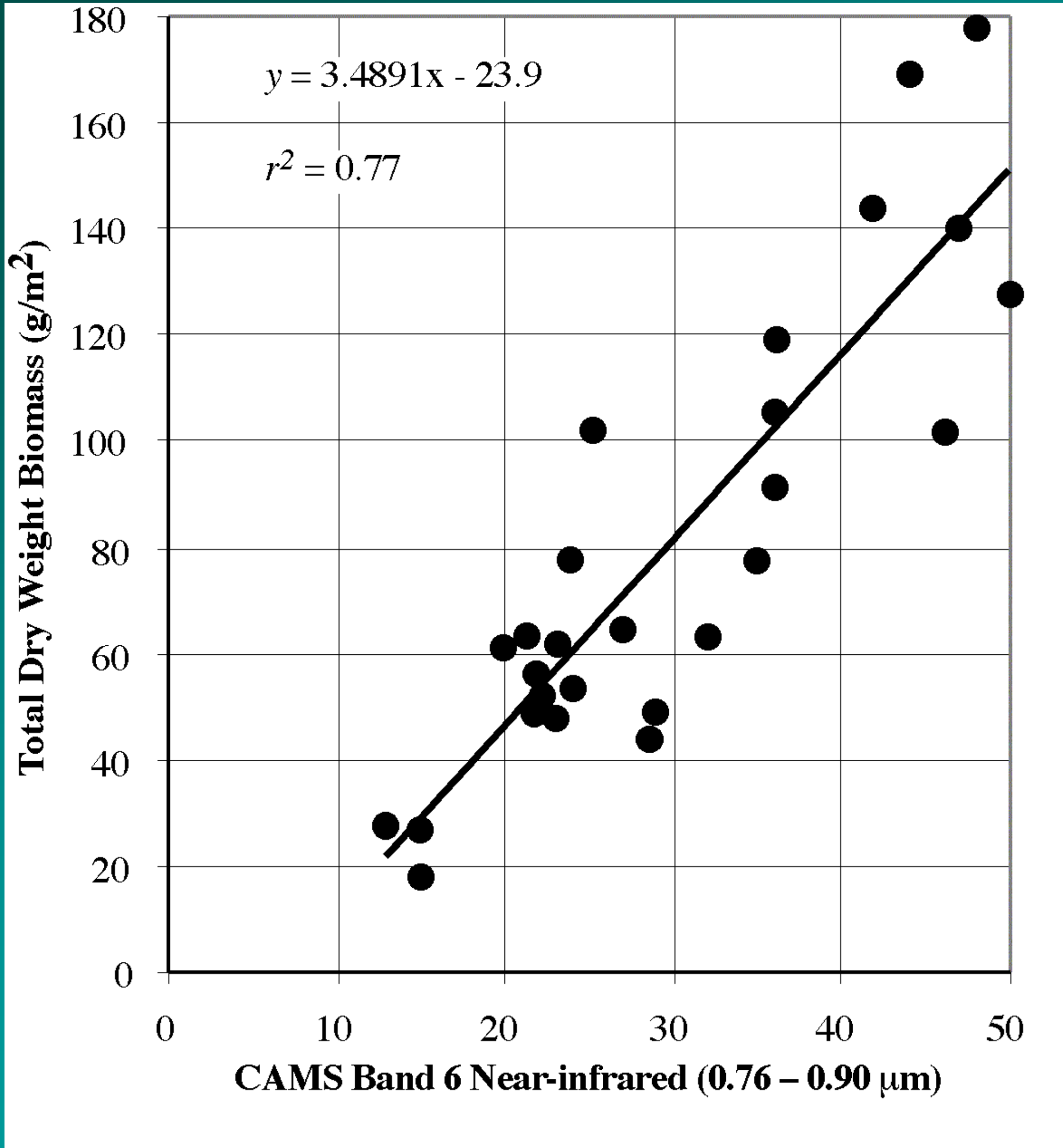

Relationship Between Calibrated Airborne Multispectral Scanner (CAMS) Band 6 Brightness Values and *in situ* Measurements of *Spartina alterniflora* Total Dry Biomass (g/m^2) at 27 Locations in Murrells Inlet, SC Obtained on August 2 and 3, 1997

Jensen, 2000

NASA Calibrated Airborne Multispectral Scanner Imagery (3 x 3 m) and Derived Biomass Map of a Portion of Murrells Inlet, South Carolina on August 2, 1997

CAMS Bands 1,2,3 (RGB)

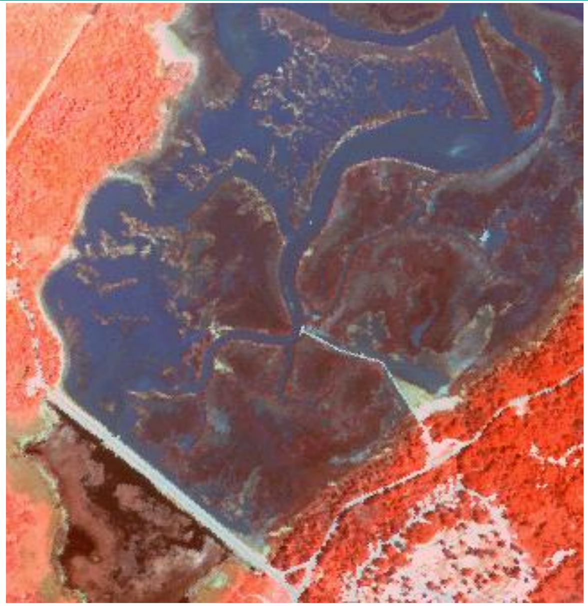

CAMS Bands 6,4,2 (RGB)

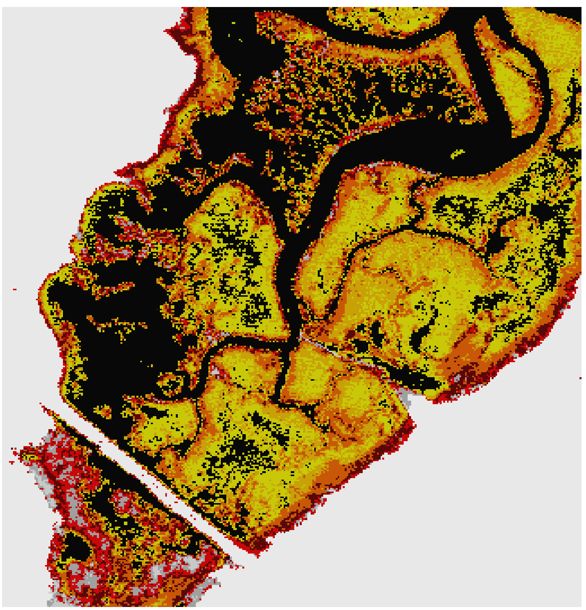

Biomass in a Portion of Murrells Inlet, SC Derived from 3 x 3 m Calibrated Airborne Multispectral Scanner (CAMS) Data Obtained on August 2, 1997

Total Biomass (grams/m^2)

- 500 - 749
- 750 - 999
- 1000 - 1499
- 1500 - 1999
- 2000 - 2499
- 2500 - 2999

Jensen, 2000

Total Above-ground Biomass in Murrells Inlet, S. C. Extracted from Calibrated Airborne Multispectral Scanner Data on August 2, 1997

Total Biomass (grams/m^2)

Yellow	500 - 749
Light orange	750 - 999
Orange	1000 - 1499
Brown	1500 - 1999
Red	2000 - 2499
Gray	2500 - 2999

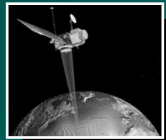

Infrared/Red Ratio Vegetation Index

The near-infrared (NIR) to red simple ratio (SR) is the first true vegetation index:

$$SR = \frac{NIR}{red}$$

It takes advantage of the inverse relationship between chlorophyll absorption of red radiant energy and increased reflectance of near-infrared energy for healthy plant canopies (Cohen, 1991) .

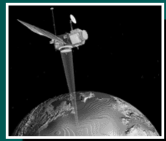

Normalized Difference Vegetation Index

The generic normalized difference vegetation index (NDVI):

$$NDVI = \frac{NIR - red}{NIR + red}$$

has provided a method of estimating net primary production over varying biome types (e.g. Lenney et al., 1996), identifying ecoregions (Ramsey et al., 1995), monitoring phenological patterns of the earth's vegetative surface, and of assessing the length of the growing season and dry-down periods (Huete and Liu, 1994).

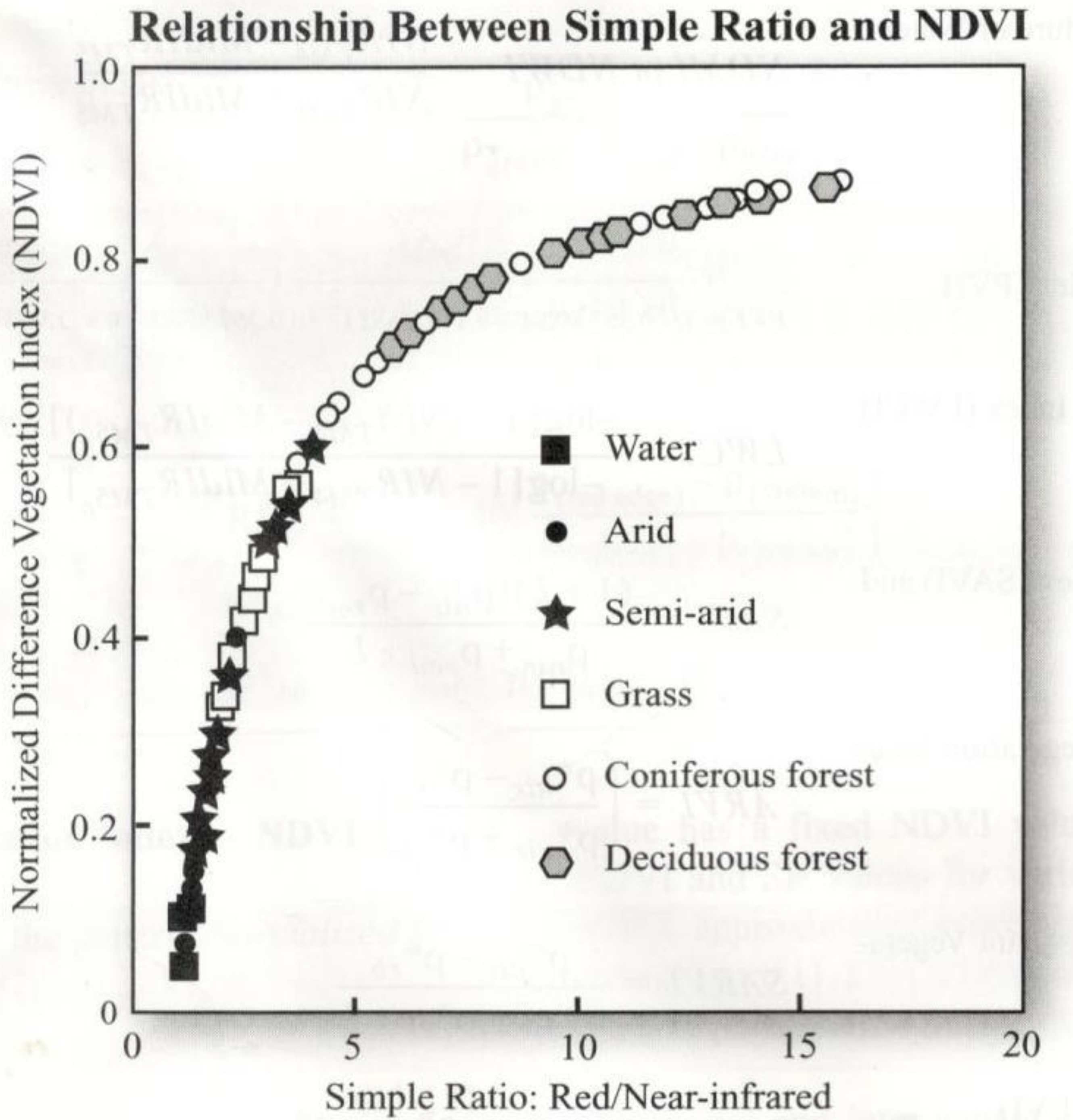
Relationship Between Simple Ratio and NDVI
Normalized Difference Vegetation Index (NDVI)
1.0
0.8
0.6
0.4
0.2
0
0
5
10
15
20
Simple Ratio: Red/Near-infrared
Water
Arid
Semi-arid
Grass
Coniferous forest
Deciduous forest

Time Series of 1984 and 1988 NDVI Measurements Derived from AVHRR Global Area Coverage (GAC) Data for the Region around El Obeid, Sudan, in Sub-Saharan Africa

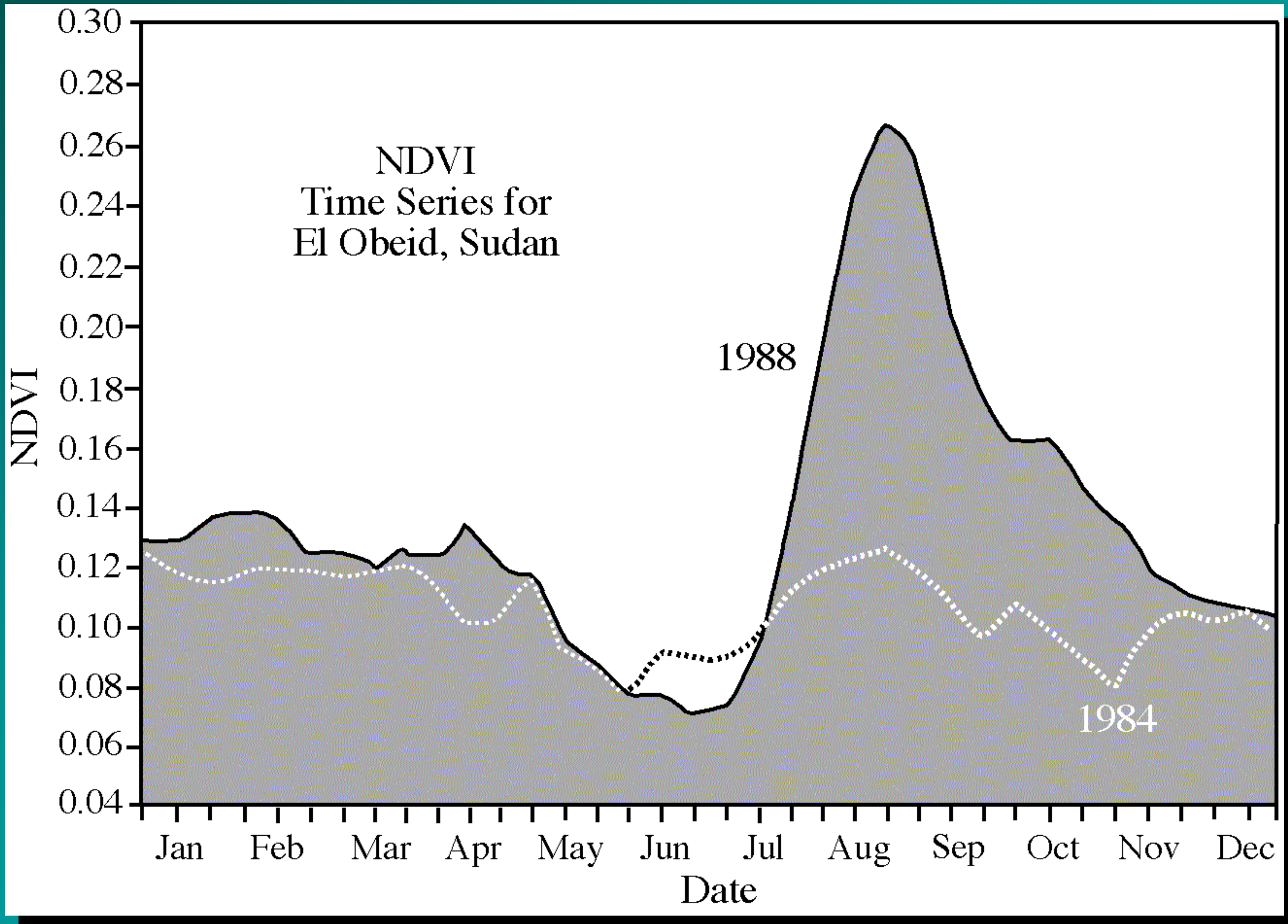

Jensen, 2000

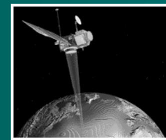

Infrared Index

An Infrared Index (II) that incorporates both near and middle-infrared bands is sensitive to changes in plant biomass and water stress in smooth cordgrass studies (Hardisky et al., 1983; 1986):

$$II = \frac{NIR_{TM\ 4} - MIR_{TM\ 5}}{NIR_{TM\ 4} + MIR_{TM\ 5}}$$

Healthy, mono-specific stands of tidal wetland such as *Spartina* often exhibit much lower reflectance in the visible (blue, green, and red) wavelengths than typical terrestrial vegetation due to the saturated tidal flat understory. In effect, the moist soil absorbs almost all energy incident to it. This is why wetland often appear surprisingly dark on traditional infrared color composites.

Jensen, 2000

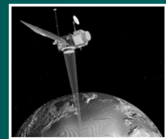

Moisture Vegetation Index

Rock et al (199) utilized a Moisture Stress Index (MSI):

$$MSI = \frac{MidIR_{TM\ 5}}{NIR_{TM\ 4}}$$

based on the Landsat Thematic Mapper near-ifnrared and middle-infrared bands

Jensen, 2000

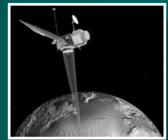

Soil Adjusted Vegetation Index (SAVI)

Recent emphasis has been given to the development of improved vegetation indices that may take advantage of calibrated hyperspectral sensor systems such as the moderate resolution imaging spectrometer - MODIS (Running et al., 1994). The improved indices incorporate a *soil adjustment factor* and/or a *blue band for atmospheric normalization*. The soil adjusted vegetation index (SAVI) introduces a soil calibration factor, *L*, to the NDVI equation to minimize soil background influences resulting from first order soil-plant spectral interactions (Huete et al., 1994):

$$SAVI = \frac{(1 + L)(NIR - red)}{NIR + red + L}$$

An *L* value of 0.5 minimizes soil brightness variations and eliminates the need for additional calibration for different soils (Huete and Liu, 1994).

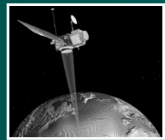

Soil and Atmospherically Adjusted Vegetation Index (SARVI)

Huete and Liu (1994) integrated the *L* function from SAVI and a blue-band normalization to derive a soil and atmospherically resistant vegetation index (SARVI) that corrects for both soil and atmospheric noise:

$$SARVI = \frac{p*nir - p*rb}{p*nir + p*rb}$$

where

$$p*rb = p*red - \gamma\left(p*blue - p*red\right)$$

The technique requires prior correction for molecular scattering and ozone absorption of the blue, red, and near-infrared remote sensor data, hence the term $p*$.

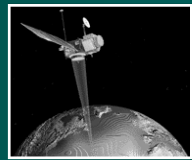

Enhanced Vegetation Index (EVI)

The MODIS Land Discipline Group proposed the *Enhanced Vegetation Index* (EVI) for use with MODIS Data:

$$EVI = \frac{p * nir - p * red}{p * nir + C_1 p * red - C_2 p * blue + L}$$

The EVI is a modified NDVI with a soil adjustment factor, *L*, and two coefficients, C_1 and C_2 which describe the use of the blue band in correction of the red band for atmsoperhic aerosol scattering. The coefficients, C_1, C_2, and *L*, are empirically determined as 6.0, 7.5, and 1.0, respectively. This algorithm has improved sensitivity to high biomass regions and improved vegetation monitoring thorugh a de-coupling of the canopy background signal and a reduction in atmospheric influences (Huete and Justice, 1999).

Landscape Ecology Metrics

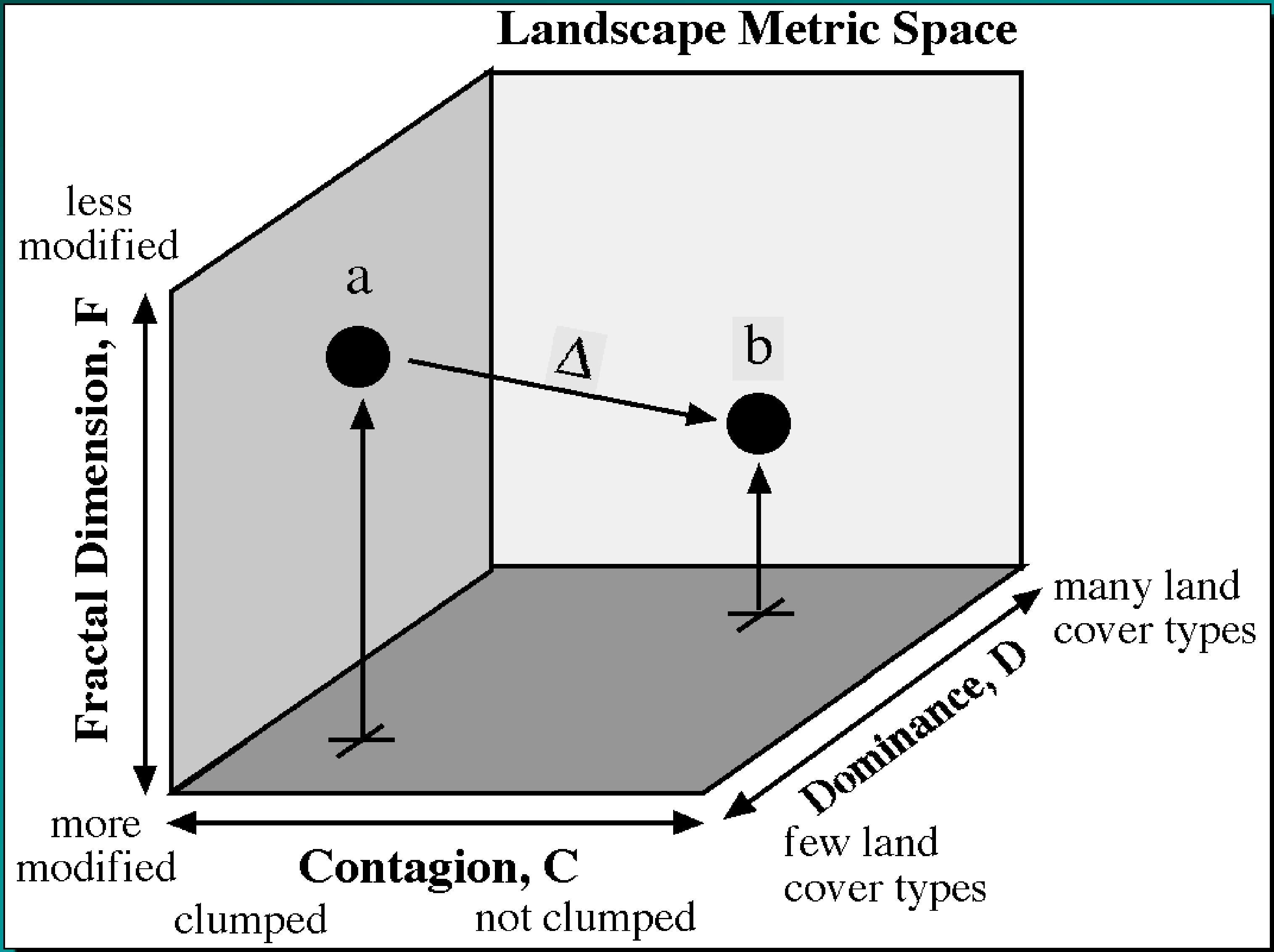

Jensen, 2000

Intermap Star3*i* X-band Radar of Wetland in Mississippi (3 x 3 m)

RADARSAT C-band (10 x 10 m)